Energy Reports 7 (2021) 3286–3301

Contents lists available at ScienceDirect

Energy Reports

journal homepage: www.elsevier.com/locate/egyr

Research paper

A new method for parameter extraction of solar photovoltaic models using gaining–sharing knowledge based algorithm

Guojiang Xiong [a,*], Lei Li [a], Ali Wagdy Mohamed [b,c], Xufeng Yuan [a], Jing Zhang [a]

[a] Guizhou Key Laboratory of Intelligent Technology in Power System, College of Electrical Engineering, Guizhou University, Guiyang, 550025, China
[b] Operations Research Department, Faculty of Graduate Studies for Statistical Research, Cairo University, Giza 12613, Egypt
[c] Wireless Intelligent Networks Center (WINC), School of Engineering and Applied Sciences, Nile University, Giza, Egypt

ARTICLE INFO

Article history:
Received 25 January 2021
Received in revised form 17 April 2021
Accepted 20 May 2021
Available online 9 June 2021

Keywords:
Solar photovoltaic
Parameter extraction
Gaining–sharing knowledge-based algorithm

ABSTRACT

For the solar photovoltaic (PV) system to operate efficiently, it is necessary to effectively establish an equivalent model of PV cell and extract the relevant unknown model parameters accurately. This paper introduces a new metaheuristic algorithm, i.e., gaining-sharing knowledge based algorithm (GSK) to solve the solar PV model parameter extraction problem. This algorithm simulates the process of knowledge acquisition and sharing in the human life cycle and is with strong competitiveness in solving optimization problems. It includes two significant phases. The first phase is the beginner–intermediate or junior acquisition and sharing stage, and the second phase is the intermediate–expert or senior acquisition and sharing stage. In order to verify the effectiveness of GSK, it is applied to five PV models including the single diode model, double diode model, and three PV modules. The influence of population size on the algorithm performance is empirically investigated. Besides, it is further compared with some other excellent metaheuristic algorithms including basic algorithms and advanced algorithms. Among the five PV models, the root mean square error values between the measured data and the calculated data of GSK are 9.8602E−04 ± 2.18E−17, 9.8280E−04 ± 8.72E−07, 2.4251E−03 ± 1.04E−09, 1.7298E−03 ± 6.25E−18, and 1.6601E−02 ± 1.44E−16, respectively. The results show that GSK has overall better robustness, convergence, and accuracy.

1. Introduction

With the aggravation of industrial pollution and excessive use of petrochemical energy, global warming, and environmental protection issues have received more attention recently. When the El Niño phenomenon, floating garbage in the ocean, smog phenomenon, land desertification, and many other phenomena caused by environmental pollution, human life has been seriously affected (Aman et al., 2015; Tooryan et al., 2020; International Energy Agency Meetings, 2020). Therefore, with the sharp increase in pollution of water sources, soil, and air, there is an urgent need for mankind to change the current energy consumption structure. As one of the vital clean energy sources with zero pollution and zero emissions, it stands to reason that solar energy should be widely used in the future life (Sharma, 2016). The Photovoltaic (PV) module is a significant part of the PV power generation system. Establishing effective models and obtaining accurate model parameters are of practical significance for tracking and controlling the actual operation of simulating PV modules and predicting PV power generation.

At present, the frequently-used PV models are single-diode and double-diode equivalent circuit models, which are used to describe the I–V characteristics of the PV cell. Sometimes, other specific PV module models will be selected for testing as needed (Jordehi, 2016; Lun et al., 2014; Li and Qiu, 2018). The *I–V* curve is a macro description of the PV cell, reflecting its output characteristic relationship. However, the equivalent circuit model reflects the internal characteristics of the PV cell. The photovoltaic power generation system is easily affected by a variety of external environmental factors, such as temperature and radiation intensity (Yang, 2020). Therefore, it needs to be optimized to use solar energy for maximum efficiency, and the effective establishment of PV models plays a vital role. In general, it is necessary to improve the accuracy of model parameter extraction to make established PV models better optimize the photovoltaic system. So that it needs to adopt efficient and accurate methods to extract various parameters of these models. We divide these methods into two types, which are analytical methods and numerical methods (Derick et al., 2017; Rusirawan and Farkas, 2014; Cuce et al., 2017; Elkholy and El-Ela, 2019).

The analysis method is principally to use the open-circuit voltage, short-circuit current, maximum power point voltage and

* Corresponding author.
E-mail address: gjxiongee@foxmail.com (G. Xiong).

https://doi.org/10.1016/j.egyr.2021.05.030

current to establish the I–V characteristic curve of the model (Al-Rashidi et al., 2011; Ortiz-Conde et al., 2016; Lin et al., 2017). The analytical methods are clarified by applying elementary functions to specific feature points of the current–voltage and power–voltage curves or transforming the equations into explicit forms through simplified and approximate methods (Phang et al., 1984). Although the method is easy to achieve, it depends to a great extent on the value of the selected point. When introducing some assumptions or approximations simplify the model, it will cause large solution errors in some cases and distortion of the extracted model parameters.

To improve the deficiencies of analysis methods, numerical methods are not limited to specific data points, so they take all the measured I–V data into account. These data reflect the connection between the actual input and output of the photovoltaic model so that it can obtain a higher degree of confidence. The numerical methods include deterministic methods and metaheuristic methods. Deterministic methods include Newton's method (Li et al., 2013), Newton–Raphson method (Chan et al., 1986), iterative curve fitting (Elbaset et al., 2014), and other methods. These methods are greatly affected by the initial parameters and easily fall into the local optimum. For some iterative methods like Newton–Raphson (NR) method and the Gauss–Seidel method (Abbassi et al., 2018a), they require a lot of computational time.

Compared with deterministic methods, metaheuristic methods have more advantages. They are to find the optimal unknown parameters based on the global optimization population algorithm. There is no restriction on the continuity of the objective function, the implementation is simple, and the robustness is strong. The methods can deal with multi-modal optimization problems more simply. Therefore, metaheuristic methods can be suitable to solve various optimization problems, such as the PV model parameter extraction problem. At present, there are many optimized metaheuristic algorithms to solve this problem, such as particle swarm optimization (PSO) (Kennedy and Eberhart, 1995), genetic algorithm (GA) (Hamid et al., 2018), differential evolution (DE) (Storn and Price, 1997),whale optimization algorithm (WOA) (Mirjalili and Lewis, 2016), teaching–learning-based optimization (TLBO) (Rao et al., 2011), harmony search (HS) (Askarzadeh and Rezazadeh, 2019), artificial bee colony (ABC) (Karaboga and Ozturk, 2011), supply–demand-based optimization (SDO) (Xiong et al., 2019a), simulated annealing (SA) (Messaoud, 2020c), cuckoo search (CS) (Srihari and Chandra, 2020), bacterial foraging algorithm (BFA) (Rajasekar et al., 2013), symbiotic organisms search (SOS) (Xiong et al., 2018c), and cat swarm optimization (CSO) (Ahmed et al., 2020). Although these algorithms can obtain good results on the PV model parameter extraction problem, most metaheuristic algorithms are still difficult to find the global optimal solution. To improve the accuracy of parameter extraction, many scholars have a lot of research on the aforementioned algorithms. Then they have obtained a more optimized algorithm based on the original algorithm, which has improved the accuracy of the results. For example, modified artificial bee colony (MABC) (Hao et al., 2013), improved adaptive differential evolution (IADE) (Wenchao et al., 2016), generalized opposition-based teaching and learning-based optimization (GOTLBO) (Chen et al., 2019), either-or teaching learning based algorithm (EOTLBO) (Xiong et al., 2020a), enhanced leader PSO (ELPSO) (Rezaee Jordehi, 2018), winner-leading competitive swarm optimizer with dynamic Gaussian mutation (WLC-SODGM) (Xiong et al., 2020b), improved whale optimization algorithm (IWOA) (Xiong et al., 2018b), and modified search strategies assisted crossover whale optimization algorithm with selection operator (MCSWOA) (Xiong et al., 2019b). The relevant experimental data of these algorithms show that the performance of the optimized algorithm has been prominently improved.

Until now, plentiful metaheuristic algorithms have been taken to solve the PV model parameter extraction problem. However, just like a coin that has two sides, different algorithms have their advantages and disadvantages. For example, GA has strong global search capabilities and can quickly search for the optimal solution randomly. But it has poor local search capability, resulting in low search efficiency in the later stage and insufficient accuracy of data extraction results. PSO is a multi-extremum function global optimization algorithm obtained by simulating the foraging behavior of birds. Its search mechanism is simple and easy to implement, but it tends to converge to the local extreme prematurely, forming a phenomenon of premature convergence. The principle of DE algorithm is simple, with fewer controlled parameters and strong robustness. However, its exploitation ability is relatively weak, resulting in slow convergence and low search accuracy. As we all know, there will always be more and better new solutions to an old problem. Therefore, for the PV model parameter extraction problem, more effective and accurate methods are also needed. Presently, scholars have proposed many improved solution methods based on traditional metaheuristic algorithms, but at the same time, more new algorithms need to be tried. In addition, it can be known from the famous non-free lunch theorem (Wolpert and Macready, 1997) that every solution method to an optimization problem may still have some room for improvement and development. Therefore, it is necessary to try new algorithms to solve more optimization problems.

Based on the above consideration, in this paper, a novel yet efficient metaheuristic algorithm of gaining–sharing knowledge based algorithm (GSK) is taken to solve the PV model parameter extraction problem. This algorithm simulates the process of knowledge acquisition and sharing in the human life cycle, and can effectively solve optimization problems. The GSK algorithm includes two significant phases, namely the beginner–intermediate or junior acquisition and sharing phase, and the intermediate–expert or senior acquisition and sharing phase (Mohamed et al., 2020). The experimental results of this algorithm in the benchmark problems have proven that, compared with other state-of-the-art meta-heuristic algorithms, GSK has strong competitiveness in convergence and robustness, especially in solving high-dimensional optimization problems. Given the excellent performance of GSK algorithm, in this paper, GSK is employed to the parameter extraction of single diode model, double diode model, and three PV module models (including the Photowatt-PWP201 module, STM6-40/36 module, and STP6-120/36 module). The impact of population size on the performance of the algorithm is researched. Finally, the experimental results are compared with other various optimization algorithms to validate the property of the GSK algorithm.

The main contributions of this paper are:

- A new metaheuristic algorithm named gaining–sharing knowledge based algorithm (GSK) is applied to solve the solar PV model parameter extraction problem.
- The influence of population size on the algorithm performance is empirically investigated.
- Five PV models are employed to verify the effectiveness of GSK. Compared with some other excellent metaheuristic algorithms including basic algorithms and advanced algorithms, the GSK algorithm is extremely competitive.

The rest of this paper is structured as follows. Section 2 describes the PV models and the objective function of the parameter extraction problem. Section 3 introduces the detailed process of the proposed GSK algorithm. The analysis and discussion of experimental results are presented in Section 4. Finally, Section 5 gives the conclusion of this paper.

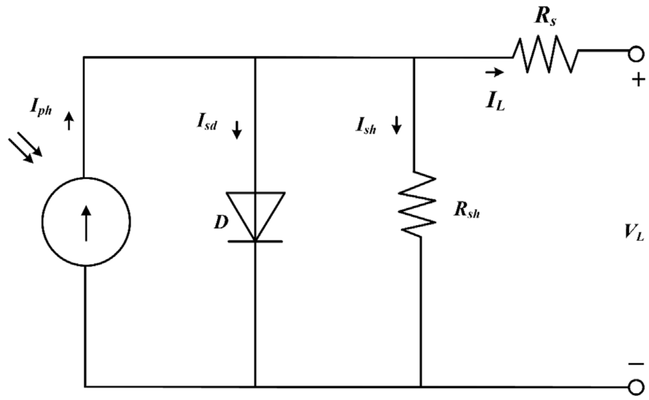

Fig. 1. Equivalent circuit of the SDM.

2. Problem formulation

The single diode model (SDM), the double diode model (DDM), and PV module models will be described in this section, as well as the objective function used in the algorithm.

2.1. Single diode model

For the SDM, as shown in Fig. 1, the output current I_L can be calculated as the following formula (Hultmann Ayala et al., 2015; Franco and Vieira, 2018; Toledo and Blanes, 2014; Ghani et al., 2014; Abbassi et al., 2018b; Stornelli et al., 2019; Messaoud, 2020a).

$$I_L = I_{ph} - I_d - I_{sh} \tag{1}$$

where I_{ph} is the total current generated by the PV cell. I_d is the diode current, and I_{sh} is shunt resistance current. Furthermore, we can get I_d from Shockley equation as follows:

$$I_d = I_{sd}\left[\exp\left(\frac{V_L + I_L \cdot R_s}{nV_t}\right) - 1\right] \tag{2}$$

where V_L is the cell output voltage. I_{sd} is the saturation current. n is the diode ideal factors. R_s is the series resistance. R_{sh} is the parallel resistance, and V_t is the junction thermal voltage defined as:

$$V_t = \frac{k \cdot T}{q} \tag{3}$$

where k is the Boltzmann constant ($1.3806503 \times 10^{-23}$ J/K). q is the electron charge ($1.60217646 \times 10^{-19}$ C), and T represents the temperature of junction in Kelvin. In addition, I_{sh} can be calculated as follows:

$$I_{sh} = \frac{V_L + I_L \cdot R_s}{R_{sh}} \tag{4}$$

Substituting Eqs. (2) and (4) into Eq. (1), I_L can be obtained as follows:

$$I_L = I_{ph} - I_{sd}\left[\exp\left(\frac{V_L + I_L \cdot R_s}{nV_t}\right) - 1\right] - \frac{V_L + I_L \cdot R_s}{R_{sh}} \tag{5}$$

From the Eq. (5), there are five unknown parameters $\left(I_{ph}, I_{sd}, R_s, R_{sh}\text{ and } n\right)$ that need to be extracted in the SDM.

2.2. Double diode model

The SDM ignores the impact of recombination current loss on circuit performance, so a more accurate model DDM is adopted to solve the loss problem. Fig. 2 is the equivalent circuit of DDM, and I_L can be calculated as follows (Brano and Ciulla, 2013; Xiong et al., 2020c; Ben, 2020; Messaoud, 2020b; Oliva et al., 2017):

$$I_L = I_{ph} - I_{sh} - I_{d1} - I_{d2} \tag{6}$$

where I_{d1} and I_{d2} is the first and second diode current , respectively. Moreover, they can be calculated as follows:

$$I_{d1} = I_{sd1}\left[\exp\left(\frac{V_L + I_L \cdot R_s}{n_1 V_t}\right) - 1\right] \tag{7}$$

$$I_{d2} = I_{sd2}\left[\exp\left(\frac{V_L + I_L \cdot R_s}{n_2 V_t}\right) - 1\right] \tag{8}$$

where n_1 and n_2 are the diode ideal factors. Through Eqs. (7) and (8), I_L can be expressed as:

$$I_L = I_{ph} - I_{sd1}\left[\exp\left(\frac{V_L + I_L \cdot R_s}{n_1 V_t}\right) - 1\right] - I_{sd2}\left[\exp\left(\frac{V_L + I_L \cdot R_s}{n_2 V_t}\right) - 1\right] - \frac{V_L + I_L \cdot R_s}{R_{sh}} \tag{9}$$

From the Eq. (9), it needs to extract seven unknown parameters $\left(I_{ph}, I_{sd1}, I_{sd2}, R_s, R_{sh}, n_1\text{ and } n_2\right)$ in the DDM.

2.3. PV module

The equivalent circuit of PV module is described in Fig. 3, which consists of $N_p \times N_s$ solar cells in series or parallel. From Eq. (10), I_L can be calculated as follows (Chin et al., 2015; Mohammed et al., 2019; Askarzadeh and Santos Coelho, 2015; Ali et al., 2016; Abbassi et al., 2019):

$$I_L = I_{ph}N_p - I_{sd}N_p\left[\exp\left(\frac{V_L + I_L R_s N_s/N_p}{nN_sV_t}\right) - 1\right] - \frac{V_L + I_L R_s N_s/N_p}{R_{sh}N_s/N_p} \tag{10}$$

Same to the SDM, there are also five unknown parameters $\left(I_{ph}, I_{sd}, R_s, R_{sh}\text{ and } n\right)$ to be extracted in the PV module.

2.4. Objective function

When extracting the undetermined parameters in the solar cell model, an objective function needs to be established to check the consistency of the established model with the actual model. Therefore, this paper regards the root mean square error (RMSE) between the measured current and the calculated current as the objective function (Ben, 2020; Messaoud, 2020b; Oliva et al., 2017):

$$RMSE\,(x) = \sqrt{\frac{1}{N}\sum_{k=1}^{N} f\,(V_L, I_L, x)^2} \tag{11}$$

where N is the number of measured data, x is a solution vector. The error functions $f\,(V_L, I_L, x)$ and the solution vectors x of the abovementioned three models can be expressed as:

$$\begin{cases} f_{SDM}\,(V_L, I_L, x) = I_{ph} - I_{sd}\left[exp\left(\frac{V_L + I_L \cdot R_s}{nV_t}\right) - 1\right] \\ \quad -\frac{V_L + I_L \cdot R_s}{R_{sh}} - I_L \\ x_{SDM} = \left(I_{ph}, I_{sd}, R_s, I_{sh}, n\right) \end{cases} \tag{12}$$

$$\begin{cases} f_{DDM}\,(V_L, I_L, x) = I_{ph} - I_{sd1}\left[exp\left(\frac{V_L + I_L \cdot R_s}{n_1V_t}\right) - 1\right] \\ -I_{sd2}\left[exp\left(\frac{V_L + I_L \cdot R_s}{n_2V_t}\right) - 1\right] - \frac{V_L + I_L \cdot R_s}{R_{sh}} - I_L \\ x_{SDM} = \left(I_{ph}, I_{sd1}, I_{sd2}, R_s, I_{sh}, n_1, n_2\right) \end{cases} \tag{13}$$

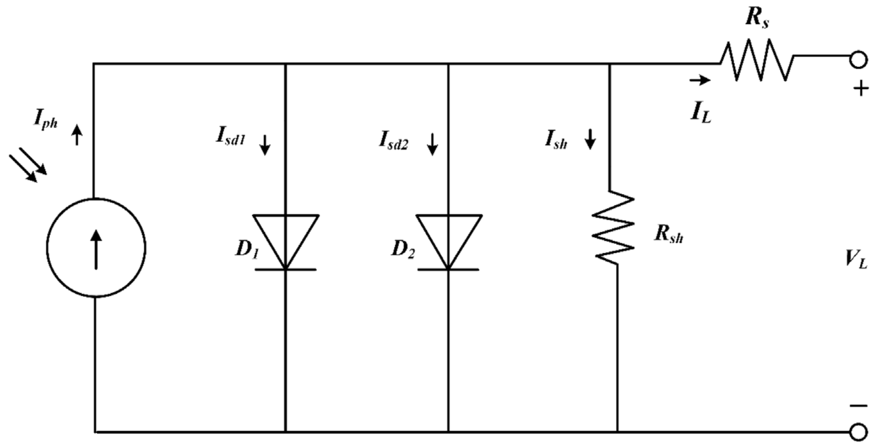

Fig. 2. Equivalent circuit of the DDM.

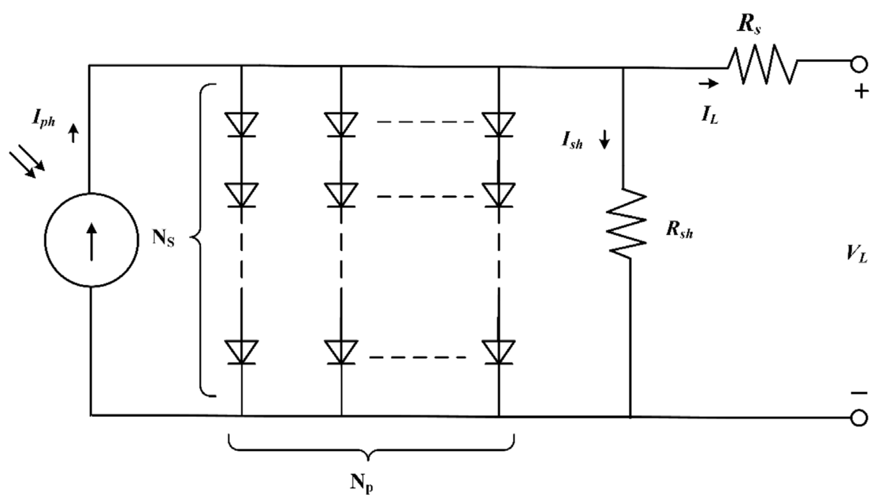

Fig. 3. Equivalent circuit of the PV module.

$$\begin{cases} f_{PV\ module}(V_L, I_L, x) = I_{ph}N_p - I_{sd}N_p\left[\exp\left(\dfrac{V_L + I_L R_s N_s/N_p}{nN_sV_t}\right) - 1\right] \\ \qquad - \dfrac{V_L + I_L R_s N_s/N_p}{R_{sh}N_s/N_p} - I_L \\ x_{PV\ module} = (I_{ph}, I_{sd}, R_s, I_{sh}, n) \end{cases} \tag{14}$$

3. Gaining-sharing knowledge based algorithm (GSK)

The gaining–sharing knowledge based algorithm is a new natural heuristic algorithm for solving continuous space optimization problems. It simulates the process of knowledge acquisition and sharing in the human life cycle. And the algorithm includes two significant phases. The first phase is the beginner–intermediate or junior acquisition and sharing stage, and the second phase is the intermediate–expert or senior acquisition and sharing stage (Mohamed et al., 2020).

The individual of a specific population is x_i, this population includes NP individuals and respective individual x_i is defined $x_i = (x_{i1}, x_{i2}, \ldots, x_{iD})$. D represents the dimension of the individual. $D_{\text{junior}phase}$ is the dimensions to be updated in each vector production process while using the junior scheme, $D_{\text{senior}phase}$ is the dimensions while using the senior scheme. According to the basic concept of knowledge acquisition and sharing, using the following nonlinear decreasing and increasing formulas to determine the number of $D_{\text{junior}phase}$ and $D_{\text{senior}phase}$:

$$D_{\text{junior}phase} = D \times (1 - \frac{G}{GEN})^K \tag{15}$$

$$D_{\text{junior}phase} = D - D_{\text{senior}phase} \tag{16}$$

where G is number of generations, GEN is the maximum number of generations, and $K > 0$ is knowledge rate.

3.1. Junior gaining-sharing knowledge phase

At this stage, every individual attempt to acquire knowledge from the nearest and trustworthy people in the small group to which he/she belongs. On account of his/her curiosity and desire, he/she also attempts to share knowledge with other individuals who are not part of the group, or who are not part of any group. Therefore, the update process for each individual using the junior schema is as follows:

1. First, according to the value of the objective function, sort all individuals in ascending order: $x_{best} \cdots x_{i-1}, x_i, x_{i+1}, \ldots, x_{worst}$
2. For x_i, choose two disparate individuals closest to him, namely the better individual (x_{i-1}) and the worse individual (x_{i+1}) than the current individual, to serve as the origin of knowledge. If x_i is globally optimal, the two individuals closest to each other are selected as follows:

```
Algorithm 1. The pseudo-code of GSK
Input: Control parameters: NP , k_f, k_r, K and p=0.1
Out: The optional solution
Set FEs = 0 and G = 1;
Initialize the population X Randomly;
Evaluate the objection function value for each individual;
FEs = FEs + NP ;
While FEs < Max_FEs do
 for i =1 to NP do
   Calculate the number of D_juniorphase with Eq.(15);
   Calculate the number of D_seniorrphase with Eq.(16);
 // Junior gaining-sharing knowledge phase
     for j =1 to D_juniorphase do
         Calculate X_i,new with Eq.(17);
     end
 //Senior gaining-sharing knowledge phase
     for j =1 to D_seniorrphase do
         Calculate X_i,new with Eq.(18);
     end
 //update each Individual
   Evaluate the objection function value for X_i,new ;
   FEs = FEs + 1 ;
    if f(X_i,new) < f(X_i) Then
       X_i = X_i,new ;
    end
 end
   G=G+1;
end while
```

Fig. 4. The pseudo code of GSK algorithm.

$(x_{best}, x_{best+1}, x_{best+2})$. If x_i is the globally worst, select the two closest individuals as follows $(x_{worst-2}, x_{worst-1}, x_{worst})$.

3. If $rand > k_r$, x_i does not change. Otherwise, the renewal process of x_i is as follows:

$$x_{i,new} = \begin{cases} x_i + k_f \cdot [(x_{i-1} - x_{i+1}) + (x_r - x_i)], & \text{if } f(x_i) > f(x_r) \\ x_i + k_f \cdot [(x_{i-1} - x_{i+1}) + (x_i - x_r)], & \text{otherwise} \end{cases} \tag{17}$$

where x_r is a randomly selected individual different from $x_{i-1}, x_i, and\ x_{i+1}$, and it is the source of sharing knowledge. $k_f > 0$ is the knowledge factor, which can control the total quantity of knowledge that the current individual gained and shared from other individuals during iterations. $k_r \in [0, 1]$ is the knowledge ratio that can control the proportion between the current experience and the experience gained during iterations.

3.2. Senior gaining-sharing knowledge phase

At this stage, the usable information and beneficial knowledge of the best, better, and worst individuals in a specific population will be utilized. Utilization refers to the influence and effect of other individuals on the current individual. Therefore, the renewal process for each individual using the senior schema as follows:

1. According to the value of the objective function, all individuals are sorted in ascending order, and then they are divided into three types: best individuals, better or middle individuals, and worst individuals, respectively.
2. Then, for x_i, from the population of the current size NP, two vectors are randomly selected from the top and bottom individuals as the acquisition portion, and a third vector is randomly selected from the middle population as the sharing portion.
3. If $rand > k_r$, x_i does not change. Otherwise, the renewal process of x_i is as follows:

$$x_{i,new} = \begin{cases} x_i + k_f \cdot \left[(x_{p-best} - x_{p-worst}) + (x_m - x_i)\right], & \text{if } f(x_i) > f(x_m) \\ x_i + k_f \cdot \left[(x_{p-best} - x_{p-worst}) + (x_i - x_m)\right], & \text{otherwise} \end{cases} \tag{18}$$

where x_{p-best} belongs to the best individuals which are the top 100p% individuals in the current population, and $x_{p-\text{worst}}$ belongs to the worst individuals which are the bottom 100p% individuals. x_m belongs to the better or middle individuals which are the middle $NP-(2\times 100p\%)$ individuals. The pseudo code and the flow chart of the GSK algorithm are shown in Figs. 4 and 5 respectively, where *FEs* is the number of fitness evaluations, *Max_FEs* is the maximum *FEs*.

4. Results and discussions

In order to verify the performance of the GSK algorithm to solve PV model parameter extraction problem, it was applied to the SDM, DDM, and three PV module models. The data set was obtained from the literature (Easwarakhanthan et al., 1986; Fathy and Rezk, 2017; Tong and Pora, 2016).

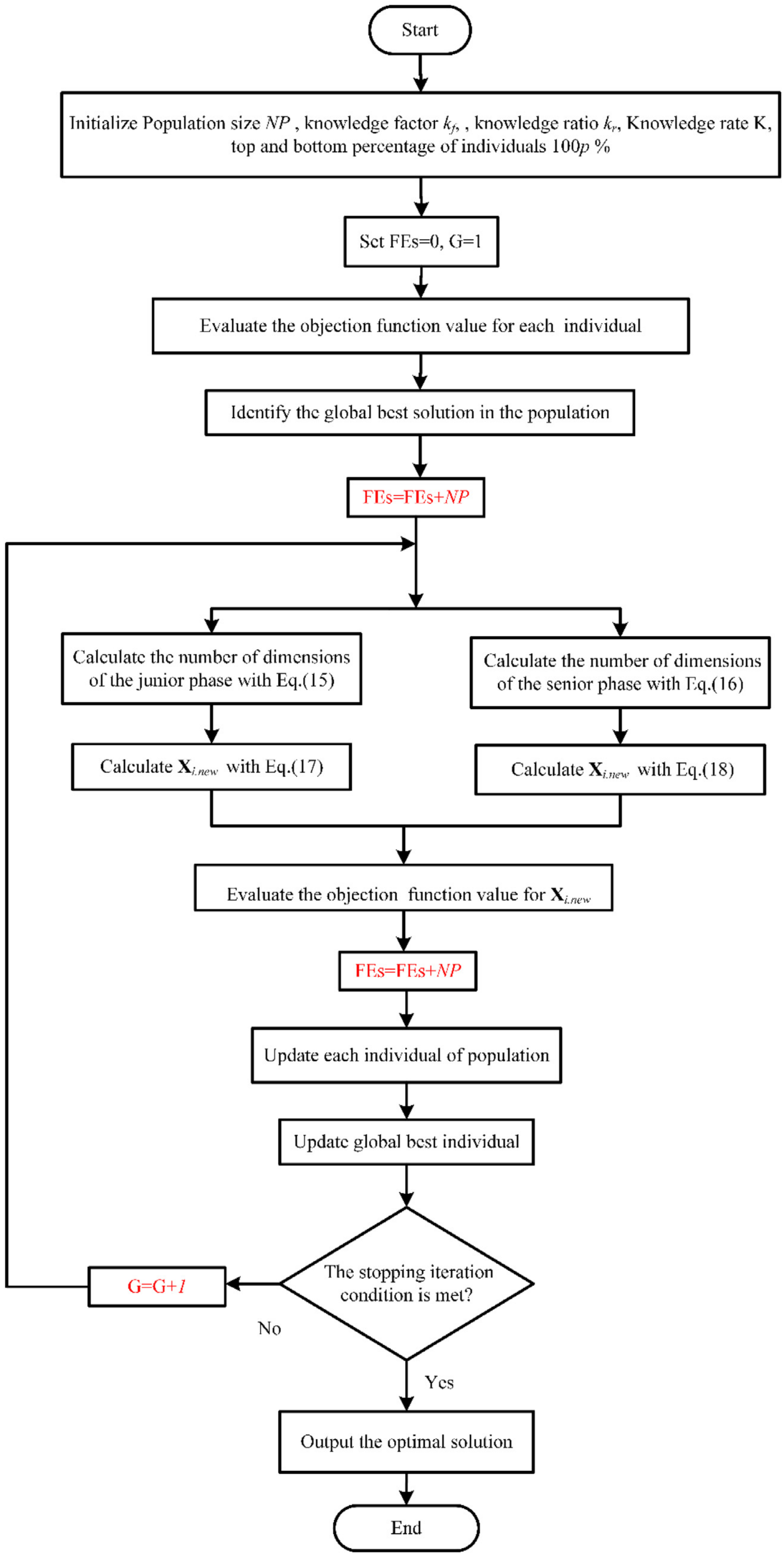

Fig. 5. The flow chart of GSK algorithm.

(1) For SDM and DDM, they were measured on commercial silicon RTC French solar cells with a diameter of 57 mm under 1000 W/m^2 irradiance at 33 °C.

(2) For PV module models, the Photowatt-PWP201 module is composed of 36 polysilicon cells connected in series under 1000 W/m^2 irradiance at 45 °C. The STM6-40/36 module is

Table 1
The parameters range of the PV models.

Parameter	Single/double diode		Photowatt-PW201		STM6-40/36		STP6-120/36	
	LB	UB	LB	UB	LB	UB	LB	UB
I_{ph} (A)	0	1	0	2	0	2	0	8
I_{sd}, I_{sd1}, I_{sd2} (μA)	0	1	0	50	0	50	0	50
R_s (Ω)	0	0.5	0	2	0	0.36	0	0.36
R_{sh} (Ω)	0	100	0	2000	0	1000	0	1500
n, n_1, n_2	1	2	1	50	1	60	1	50

Table 2
Parameter settings of different algorithms.

Algorithm	Parameter setting
GSK	$NP = 30$, $k_r = 0.9$, $k_f = 0.5$, $K = 10$, $p = 0.1$
ABC	$NP = 30$, FoodNumber = 15, Limit = 100
BBO	$NP = 30$, MutationProb = 0.1
DE	$NP = 30$, $F = 0.5$, $CR = 0.9$
JAYA	$NP = 30$, rand$_1$ = rand$_2$ = rand(0,1)
PSO	$NP = 30$, $C_1 = C2 = 2$
WOA	$NP = 30$, $r_1 = r2 = p =$ rand(0,1)
TLBO	$NP = 30$, $T_F =$ round(1 + rand(0,1))
ITLBO (Rao et al., 2011)	$NP = 50$
GOTLBO (Chen et al., 2019)	$NP = 50$, $Jr = 1.00$
SATLBO (Simon, 2008)	$NP = 40$
RTLBO (Tong and Pora, 2016)	$NP = 40$
BSA (Rao and Patel, 2013)	$NP = 50$, Mixrate = 1.00
TLABC (Civicioglu, 2013)	$NP = 50$, Scale factor F = rand(0,1)

composed of 36 monocrystalline silicon cells connected in series under 1000 W/m^2 irradiance at 51 °C. And the STP6-120/36 module is composed of 36 monocrystalline silicon cells connected in series under 1000 W/m^2 irradiance at 55 °C.

The search range of these model parameters is shown in Table 1. Besides, the GSK algorithm is compared with seven basic metaheuristic algorithms and nine advanced optimization algorithms, which are artificial bee colony (ABC) (Karaboga and Ozturk, 2011), biogeography based optimization (BBO) (Simon, 2008), differential evolution (DE) (Storn and Price, 1997), JAYA algorithm (Rao, 2016), particle swarm optimization (PSO) (Kennedy and Eberhart, 1995), whale optimization algorithm (WOA) (Mirjalili and Lewis, 2016), teaching–learning-based optimization (TLBO) (Rao et al., 2011), generalized oppositional teaching–learning-based optimization (GOTLBO) (Chen et al., 2019), improved teaching–learning-based optimization (ITLBO) (Rao and Patel, 2013), ranking teaching–learning-based optimization (RTLBO) (Xiong et al., 2018a), self-adaptive teaching–learning-based optimization (SATLBO) (Yu et al., 2017a), teaching–learning-based optimization with the learning experience of other learners (LETLBO) (Zou et al., 2015), backtracking search optimization algorithm (BSA) (Civicioglu, 2013), teaching–learning-based artificial bee colony (TLABC) (Chen et al., 2018), improved whale optimization algorithm (IWOA) (Xiong et al., 2018b), and improved JAYA optimization algorithm (IJAYA) (Yu et al., 2017b). At the same time, each algorithm runs individually 30 times in Matlab2106b. The parameter settings of these algorithms are given in Table 2, which are derived from their respective original literature. We set different *Max_FEs* values for different models. *Max_FEs* is 50 000 for the DDM which has seven parameters and 30 000 for the other PV models which has five parameters.

4.1. Influence of population size on GSK

When the meta-heuristic algorithm is taken to solve the PV model parameter extraction problem, the determination of the population size is one of the critical steps. Choosing the appropriate population size can more effectively help the corresponding algorithm show better performance. Therefore, this section focuses on this problem and studies the influence of different NP values on the GSK algorithm in the PV model parameter extraction problem. Test with NP set to 10, 20, 30, 40, and 50, respectively, and keep the value of *Max_FEs* the same as above. The experimental results are shown in Table 3. It can be seen that NP does affect the algorithm performance of GSK. In the DDM, the SDM, the Photowatt-PWP201 module, and the STM6-40/36 module, the best RMSE value results are obtained when NP = 30. In the STP6-120/36 module, GSK have the best performance when NP = 20. However, it is worth noting that this result is very close to that obtained when NP = 30. And when NP = 10, the RMSE value obtained is worse than the value when NP = 20. And when NP > 30, with the increase in the number of NP, the performance of GSK becomes worse and worse. The reasons of the results are explained in the following analysis:

(1) It is well known that the parameter extraction problem of PV models is a typical multi-modal optimization problem, and there are multiple local minima in the search process. When the population size is small, the number of iterations will increase significantly because the given value of *Max_FEs* remains unchanged. But at the same time, it also causes the decrease of population diversity and affects the range of movement between individuals. It is easy for all individuals to fall into a certain local optimal value in large quantities, which results in premature convergence. Therefore, when NP = 10, the RMSE value of the GSK algorithm is not ideal.
(2) In addition, the PV model parameter extraction is also a low dimensional optimization problem. Therefore, it is not necessary to set it in this way even if a larger population size can improve the population diversity. Because it is not good for convergence when all the individuals are spread out over the entire search area. Moreover, the larger the population size is, the more times of fitness evaluation are needed, leading to a significant reduction in the number of iterations, which is disadvantageous to the solution of such optimization problems. So, with the increase in the number of NP, the performance of GSK becomes worse and worse.

In order to make the GSK algorithm show better performance in the PV model parameter extraction problems, the *NP* value is set to 30 for testing in this paper.

4.2. Results on the SDM

When we apply the abovementioned algorithms to the parameter extraction of the SDM, the unknown extracted parameters of these algorithms are shown in Table 4. It can be seen that the parameter values extracted by these algorithms have little difference in the SDM. At the same time, Fig. 6 shows the I–V and P-V characteristic curves of the GSK algorithm. It can be obtained that the calculated current obtained by this algorithm has a high degree of fitting with the measured current.

The performance of the algorithm in SDM is validated by calculating different types of RMSE values (the minimum, maximum,

Table 3
The RMSE values (Mean ± Std).of the GSK algorithm under different population sizes in different PV models.

NP	SDM	DDM	Photowatt-PW201	STM6-40/36	STP6-120/36
10	9.8602E−04 ± 2.91E−16	9.8402E−04 ± 1.67E−06	2.4251E−03 ± 7.33E−05	1.7298E−03 ± 4.17E−17	1.6601E−02 ± 1.35E−15
20	9.8602E−04 ± 3.09E−17	9.8300E−04 ± 1.13E−06	2.4251E−03 ± 8.61E−09	1.7298E−03 ± 7.30E−18	**1.6601E−02 ± 9.61E−17**
30	**9.8602E−04 ± 2.18E−17**	**9.8280E−04 ± 8.72E−07**	**2.4251E−03 ± 1.04E−09**	**1.7298E−03 ± 6.25E−18**	1.6601E−02 ± 1.44E−16
40	9.8602E−04 ± 2.82E−17	9.8325E−04 ± 1.41E−06	2.4251E−03 ± 2.71E−09	1.7298E−03 ± 1.45E−12	1.6601E−02 ± 1.12E−11
50	9.8602E−04 ± 1.44E−15	9.8704E−04 ± 1.09E−05	2.4251E−03 ± 5.36E−05	1.7298E−03 ± 2.63E−09	1.6601E−02 ± 1.80E−07

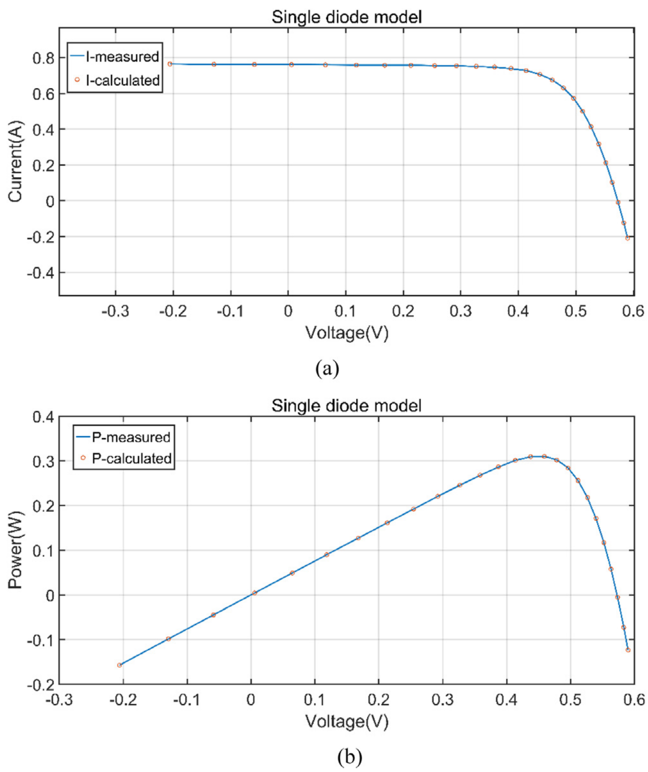

Fig. 6. The characteristic curve of the GSK algorithm for the SDM. (a) I–V (b) P-V.

Table 4
Comparison among different parameter extraction algorithms on the single diode model.

Algorithm	Parameter				
	I_{ph} (A)	I_{sd} (μA)	R_s (Ω)	R_{sh} (Ω)	n
GSK	0.7608	0.3231	0.0364	53.7227	1.4812
ABC	0.7606	0.3174	0.0365	57.0609	1.4790
BBO	0.7608	0.2839	0.0373	51.7597	1.4681
DE	0.7608	0.3231	0.0364	53.7185	1.4812
JAYA	0.7608	0.3152	0.0367	55.3139	1.4770
PSO	0.7608	0.3412	0.0362	55.0458	1.4868
WOA	0.7608	0.3241	0.0358	55.3054	1.4843
TLBO	0.7608	0.3325	0.0363	55.3129	1.4839
GOTLBO	0.7608	0.3420	0.0362	53.8599	1.4870
ITLBO	0.7608	0.3230	0.0364	53.7187	1.4812
RTLBO	0.7608	0.3423	0.0361	55.3065	1.4871
SATLBO	0.7608	0.3423	0.0361	55.3462	1.4870
LETLBO	0.7608	0.3322	0.0364	53.6655	1.4809
BSA	0.7608	0.3257	0.0363	54.3242	1.4865
TLABC	0.7608	0.3231	0.0364	53.7164	1.4812
IWOA	0.7608	0.3232	0.0364	53.7185	1.4812
IJAYA	0.7608	0.3228	0.0364	53.7959	1.4811

mean, and standard deviation values). Table 5 is the experimental result of nine abovementioned optimization algorithms. In the case of the *Max_FEs* value of 30 000, it is worth mentioning that GSK can obtain the smallest standard deviation value (2.18E−17). In the other three indicators, GSK, DE, and ITLBO get the smallest RMSE value (9.8602E−04). It indicates that the GSK algorithm has stronger competitiveness in the parameter extraction of the SDM. Moreover, Fig. 7 shows the convergence curve of the SDM to verify the convergence performance of GSK. It can be seen that DE has the fastest convergence speed than other algorithms in the initial stages. However, it falls into local optima quickly. GSK and ITLBO converge to the smallest RMSE value eventually. It shows that the GSK algorithm has superior convergence performance in the SDM.

Table 5
RMSE values of different algorithms in the single diode model.

Algorithm	RMSE			
	Best	Worst	Mean	Std
GSK	**9.8602E−04**	**9.8602E−04**	**9.8602E−04**	**2.18E−17**
ABC	1.0025E−03	2.4364E−03	1.5873E−03	4.06E−04
BBO	1.2299E−03	4.3254E−03	2.4391E−03	7.29E−04
DE	**9.8602E−04**	1.3410E−03	1.0096E−03	6.72E−05
JAYA	1.0497E−03	1.5041E−03	1.2127E−03	1.29E−04
PSO	9.8761E−04	2.3586E−03	1.4460E−03	3.72E−04
WOA	1.1575E−03	1.8070E−02	4.1352E−03	4.23E−03
TLBO	9.8964E−04	1.9354E−03	1.3236E−03	2.37E−04
GOTLBO	9.8760E−04	1.7095E−03	1.0949E−03	1.36E−04
ITLBO	**9.8602E−04**	**9.8602E−04**	**9.8602E−04**	4.57E−17
RTLBO	9.8604E−04	1.0808E−03	1.0057E−03	3.06E−05
SATLBO	9.8932E−04	1.7540E−03	1.2426E−03	1.91E−04
BSA	9.9004E−04	1.5031E−03	1.1423E−03	1.29E−04
TLABC	9.8602E−04	1.0481E−03	9.9811E−04	1.76E−05

Then we select five algorithms with better RMSE values from Table 5 to compare with GSK, which are DE, GOTLBO, RTLBO, ITLBO, and TLABC respectively. And Table 6 is the calculated current data obtained by using the parameters extracted by these algorithms. The corresponding individual absolute error (IAE) values are calculated by comparing the measured current and the calculated current of each algorithm. The IAE value of the GSK algorithm is less than other algorithms, indicating that the algorithm has a higher accuracy of parameter extraction on the SDM.

4.3. Results on the DDM

For the DDM, the extracted parameters of these algorithms are shown in Table 7, and Fig. 8 shows the I–V and P-V characteristic curves of the GSK algorithm. It can be seen that the calculated current obtained by the algorithm is also highly fitted to the measured current in the DDM.

Table 8 is the RMSE value results of nine abovementioned optimization algorithms. In the case of the *Max_FEs* value of 50 000, GSK, ITLBO, and TLABC can get the best RMSE value (9.8248e−04). However, GSK can obtain the smallest values in the other three indicators. What is noteworthy is that GSK can obtain the smallest mean value (9.8280E−04) and the smallest standard deviation value (8.72E−07). It also indicates that the GSK algorithm has better performance in the parameter extraction of the SDM. Moreover, Fig. 9 shows the convergence curve of the DDM to verify the convergence performance of GSK. It can be seen that DE and GOTLBO have a faster convergence speed than other algorithms in the initial stages. However, they fall into local

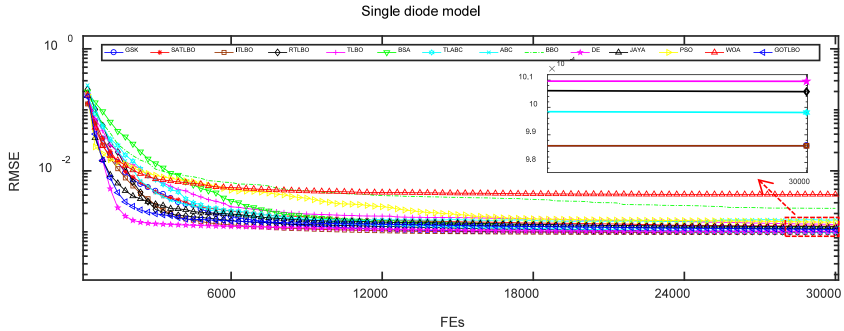

Fig. 7. The convergence curve for the SDM.

Table 6
The IAE results for the single diode model.

Item	V_L (V)	$I_{L\,measured}$ (A)	$I_{L\,calculated}$ (A)					
			GSK	DE	GOTLBO	ITLBO	RTLBO	TLABC
1	−0.2057	0.7640	0.7641	0.7641	0.764	0.7641	0.7641	0.7641
2	−0.1291	0.7620	0.7627	0.7627	0.7626	0.7627	0.7626	0.7627
3	−0.0588	0.7605	0.7614	0.7614	0.7614	0.7614	0.7614	0.7614
4	0.0057	0.7605	0.7602	0.7602	0.7602	0.7602	0.7602	0.7602
5	0.0646	0.7600	0.7591	0.7591	0.7591	0.7591	0.7591	0.7591
6	0.1185	0.7590	0.7581	0.7581	0.7581	0.7581	0.7581	0.7581
7	0.1678	0.7570	0.7571	0.7571	0.7572	0.7571	0.7571	0.7571
8	0.2132	0.7570	0.7562	0.7562	0.7563	0.7562	0.7562	0.7562
9	0.2545	0.7555	0.7551	0.7551	0.7553	0.7551	0.7551	0.7551
10	0.2924	0.7540	0.7537	0.7537	0.7539	0.7537	0.7537	0.7537
11	0.3269	0.7505	0.7514	0.7514	0.7516	0.7514	0.7514	0.7514
12	0.3585	0.7465	0.7474	0.7474	0.7475	0.7474	0.7474	0.7473
13	0.3873	0.7385	0.7401	0.7401	0.7402	0.7401	0.7401	0.7400
14	0.4137	0.7280	0.7274	0.7274	0.7274	0.7274	0.7274	0.7272
15	0.4373	0.7065	0.7070	0.7071	0.7069	0.7070	0.7070	0.7067
16	0.4590	0.6755	0.6753	0.6752	0.6752	0.6753	0.6753	0.6749
17	0.4784	0.6320	0.6309	0.6309	0.6389	0.6309	0.6309	0.6306
18	0.4960	0.5730	0.5720	0.5719	0.5720	0.5720	0.5721	0.5712
19	0.5119	0.4990	0.4994	0.4993	0.4995	0.4992	0.4995	0.4994
20	0.5265	0.4130	0.4134	0.4134	0.4135	0.4135	0.4135	0.4133
21	0.5398	0.3165	0.3172	0.3172	0.3173	0.3172	0.3172	0.3171
22	0.5521	0.2120	0.2120	0.2121	0.2122	0.2121	0.2122	0.2111
23	0.5633	0.1035	0.1027	0.1026	0.1027	0.1027	0.1082	0.1021
24	0.5736	−0.0100	−0.0093	−0.0091	−0.0093	−0.0092	−0.0091	−0.0089
25	0.5833	−0.1230	−0.1244	−0.1243	−0.1246	−0.1243	−0.1242	−0.1242
26	0.5900	−0.2100	−0.2092	−0.2090	−0.2096	−0.2091	−0.2090	−0.2090
	$\sum IAE$		0.0174	0.0181	0.0233	0.0175	0.0217	0.0203

Table 7
Comparison among different parameter extraction algorithms on the double diode model.

Algorithm	Parameter						
	I_{ph} (A)	I_{sd1} (μA)	I_{sd2} (μA)	R_s (Ω)	Rsh (Ω)	n_1	n_2
GSK	0.7608	0.2595	0.4791	0.0366	54.9330	1.4627	1.9983
ABC	0.7608	0.3811	0.8456	0.0367	55.2881	1.4747	1.9374
BBO	0.7609	0.2848	0.3645	0.0332	61.9024	1.5431	1.5654
DE	0.7608	0.3564	0..5762	0.0366	54.3994	1.4575	1.9974
JAYA	0.7608	0.3362	0.2451	0.0361	50.9434	1.4856	1.9609
PSO	0.7608	0.2568	0.3154	0.0366	53.9064	1.4617	1.9063
WOA	0.7608	0.2747	0.3032	0.0366	53.8598	1.4753	1.8203
TLBO	0.7608	0.1423	0.3365	0.0362	54.8506	1.4462	1.9878
GOTLBO	0.7608	0.3410	0.2634	0.0345	54.4147	1.4638	1.9910
ITLBO	0.7608	0.3204	0.8451	0.0364	53.7216	1.4743	1.7892
RTLBO	0.7608	0.2299	0.8527	0.0363	49.0850	1.4552	1.9614
SATLBO	0.7608	0.2895	0.2596	0.0364	54.9758	1.4723	1.9653
LETLBO	0.7608	0.1137	0.3032	0.0364	54.0688	1.4760	1.9284
BSA	0.7608	0.2496	0.4137	0.0363	54.4915	1.4618	1.8707
TLABC	0.7608	0.4239	0.2401	0.0367	54.6680	1.4567	1.9075
IWOA	0.7608	0.3232	0.4366	0.0364	53.7185	1.4812	1.9994
IJAYA	0.7608	0.0050	0.7509	0.0376	77.8519	1.4811	1.6247

optima when $FEs = 30\,000$. As the iteration progresses, GSK can get more excellent convergence effects than them.

Then we also select five algorithms with better RMSE values from Table 8 to compare with GSK, which are DE, GOTLBO, RTLBO, ITLBO, and TLABC respectively. Table 9 is the calculated current data obtained by using the extracted parameters by these algorithms. It is obvious that the IAE values of GSK are relatively

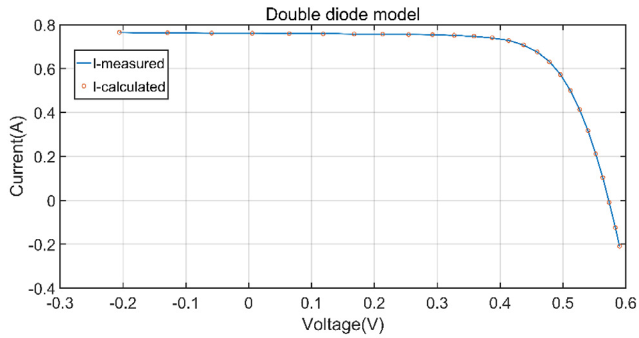

(a)

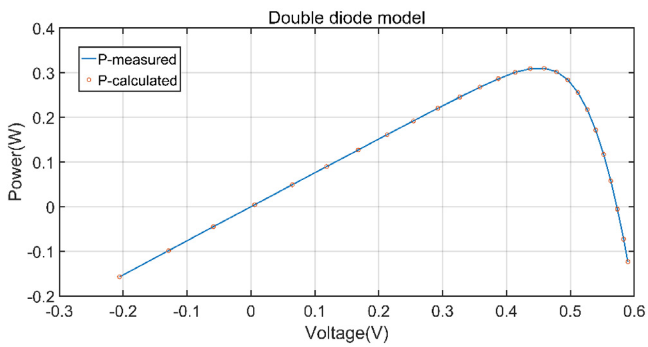

(b)

Fig. 8. The characteristic curve of the GSK algorithm for the DDM. (a) I–V (b) P-V.

Table 8
The RMSE values of different algorithms in the double diode model.

Algorithm	RMSE			
	Best	Worst	Mean	Std
GSK	**9.8248e−04**	**9.8602E−04**	**9.8280E−04**	**8.72E−07**
ABC	1.0088E−03	1.7499E−03	1.9687E−03	2.11E−04
BBO	1.6461E−03	4.3518E−03	2.5094E−03	6.61E−04
DE	9.8263E−04	1.1974E−03	9.9258E−04	3.87E−05
JAYA	1.0001E−03	1.5538E−03	1.2176E−03	1.54E−04
PSO	9.8469E−04	1.9228E−03	1.3274E−03	3.13E−04
WOA	9.9056E−04	1.1420E−02	3.0638E−03	2.35E−03
TLBO	9.8364E−04	2.9946E−03	1.4304E−03	4.72E−04
GOTLBO	9.8317E−04	1.2683E−03	1.0435E−03	9.28E−05
ITLBO	**9.8248e−04**	9.8683E−04	9.8510E−04	1.33E−06
RTLBO	9.8272E−04	1.0874E−03	9.9286E−04	1.95E−05
SATLBO	9.8614e−04	2.0579E−03	1.2316E−03	2.44E−04
BSA	9.9094E−04	1.3241E−03	1.0759E−03	8.99E−05
TLABC	**9.8248E−04**	9.9220E−04	9.8545E−04	2.06E−06

small, indicating that the GSK algorithm has a higher accuracy of parameter extraction on the DDM.

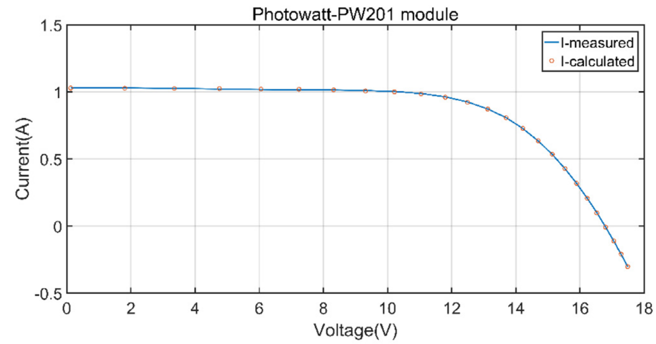

(a)

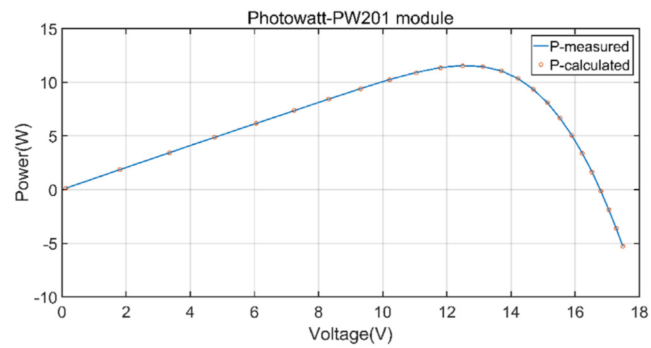

(b)

Fig. 10. The characteristic curve of the GSK algorithm for the Photowatt-PW201 module. (a) I–V (b) P-V.

4.4. Results on the PV modules

Tables 10, 11, 12 respectively show the optimal extracted parameter values of the Photowatt-PW201 module, the STM6-40/36 module, and the STP6-120/36 module. And Figs. 10, 11, 12 are the I–V and P-V characteristic curves of GSK, which show that the calculated current obtained by this algorithm is highly fitted to the measured current in these PV modules.

Tables 13, 14, 15 are the results of the RMSE values of the aforementioned optimization algorithms, and Figs. 13, 14, 15 are their convergence curves. We can get the analysis as follows:

- In the Photowatt-PW201 module, GSK, DE, ITLBO, RTLBO and TLABC can get the best RMSE value (2.4251E−03), GSK and ITLBO get the smallest worst and mean values (2.4251E−03). Though ITLBO can obtain the smallest standard deviation value (3.46E−14), Table 13 shows that there is little difference between GSK and ITLBO. Then from Fig. 13,

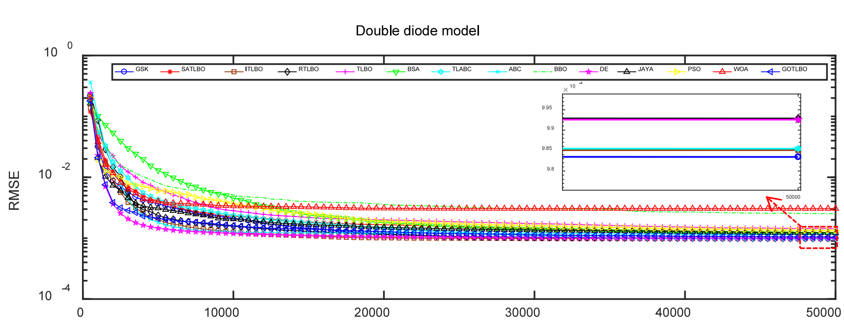

Fig. 9. The convergence curve for the DDM.

Table 9
The IAE results for the double diode model.

Item	V_L (V)	$I_{L\,measured}$ (A)	$I_{L\,calculated}$ (A)					
			GSK	DE	GOTLBO	ITLBO	RTLBO	TLABC
1	−0.2057	0.7640	0.7641	0.7640	0.7641	0.7641	0.7640	0.7641
2	−0.1291	0.7620	0.7627	0.7626	0.7626	0.7627	0.7626	0.7627
3	−0.0588	0.7605	0.7614	0.7614	0.7614	0.7614	0.7614	0.7614
4	0.0057	0.7605	0.7602	0.7602	0.7602	0.7602	0.7601	0.7602
5	0.0646	0.7600	0.7591	0.7591	0.7591	0.7591	0.7589	0.7591
6	0.1185	0.7590	0.7581	0.7581	0.7581	0.7581	0.7578	0.7581
7	0.1678	0.7570	0.7571	0.7572	0.7571	0.7571	0.7567	0.7571
8	0.2132	0.7570	0.7562	0.7563	0.7562	0.7562	0.7557	0.7562
9	0.2545	0.7555	0.7552	0.7553	0.7551	0.7552	0.7545	0.7552
10	0.2924	0.7540	0.7538	0.7538	0.7536	0.7538	0.7529	0.7538
11	0.3269	0.7505	0.7514	0.7515	0.7512	0.7514	0.7505	0.7514
12	0.3585	0.7465	0.7473	0.7474	0.7466	0.7473	0.7462	0.7473
13	0.3873	0.7385	0.7401	0.7402	0.7381	0.7401	0.7387	0.7401
14	0.4137	0.7280	0.7273	0.7274	0.7254	0.7273	0.7258	0.7273
15	0.4373	0.7065	0.7071	0.7069	0.7044	0.7072	0.7052	0.7073
16	0.4590	0.6755	0.6754	0.6752	0.6731	0.6754	0.6735	0.6749
17	0.4784	0.6320	0.6310	0.6389	0.6291	0.6310	0.6293	0.6309
18	0.4960	0.5730	0.5721	0.5720	0.5695	0.5717	0.5707	0.5719
19	0.5119	0.4990	0.4995	0.4995	0.4979	0.4995	0.4985	0.4998
20	0.5265	0.4130	0.4135	0.4134	0.4127	0.4136	0.4138	0.4138
21	0.5398	0.3165	0.3173	0.3171	0.3149	0.3174	0.3170	0.3172
22	0.5521	0.2120	0.2121	0.2119	0.2113	0.2121	0.2125	0.2124
23	0.5633	0.1035	0.1028	0.1026	0.1026	0.1026	0.1031	0.1025
24	0.5736	−0.0100	−0.0092	−0.0095	−0.0094	−0.0114	−0.0088	−0.0091
25	0.5833	−0.1230	−0.1243	−0.1246	−0.1247	−0.1245	−0.1238	−0.1244
26	0.5900	−0.2100	−0.2090	−0.2095	−0.2083	−0.2091	−0.2086	−0.2091
	$\sum IAE$		0.0175	0.0228	0.0287	0.0191	0.0250	0.0197

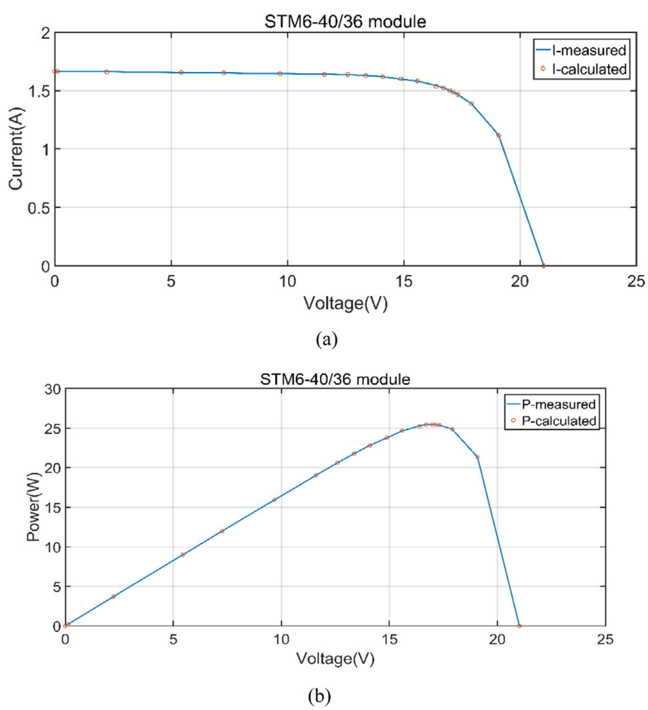

Fig. 11. The characteristic curve of the GSK algorithm for the STM6-40/36 module. (a) I–V (b) P-V.

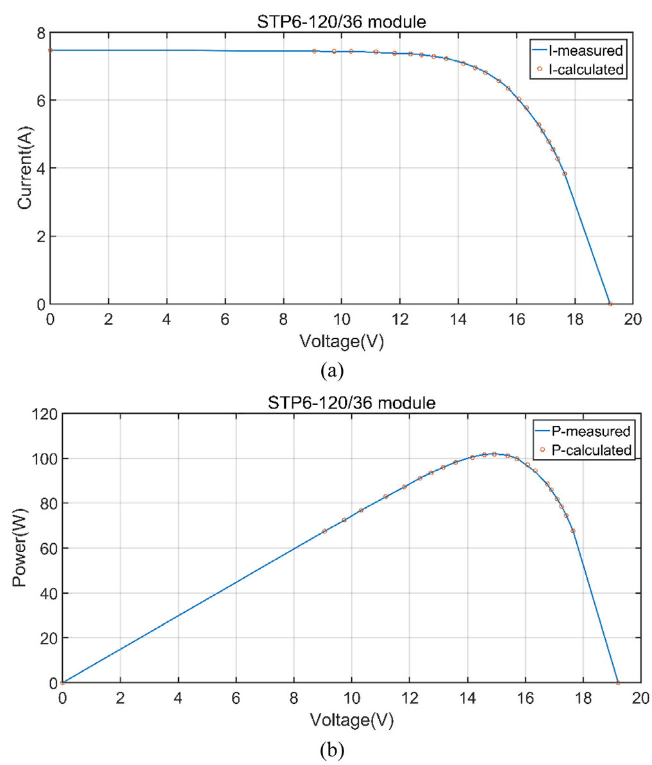

Fig. 12. The characteristic curve of the GSK algorithm for the STP6-120/36 module. (a) I–V (b) P-.

GSK has the fastest rate of convergence. Finally, GSK and ITLBO both get excellent convergence results.

- In the STM6-40/36 module, GSK, ITLBO, RTLBO and TLABC can get the best RMSE value (1.7298E−03), GSK gets the smallest worst and mean values (1.7298E−03). It is worth mentioning that GSK can obtain the smallest standard deviation value (6.25E−18). Then from Fig. 14, GSK has the fastest rate of convergence and get more excellent convergence results than other algorithms.
- In the STP6-120/36 module, GSK and ITLBO can get the best RMSE value (1.6601E−02). Moreover, GSK gets the smallest worst and mean value (1.6601E−02), it is worth mentioning that GSK can obtain the optimal standard deviation values

Table 10
Extracted parameters for the Photowatt-PW201 module.

Algorithm	Parameter				
	I_{ph} (A)	I_{sd} (μA)	R_s (Ω)	R_{sh} (Ω)	n
GSK	1.0305	3.4823	1.2013	981.9823	48.6428
ABC	1.0281	4.9125	1.1671	990.8662	49.9917
BBO	1.0360	3.2658	1.2545	994.8378	48.3836
DE	1.0305	3.4823	1.2012	981.9823	48.6848
JAYA	1.0304	3.5622	1.1967	970.1747	48.7315
PSO	1.0305	3.4258	1.2032	971.2958	48.5756
WOA	1.0127	4.5112	1.1429	949.7849	49.9993
TLBO	1.0306	3.4426	1.2027	967.7212	48.5913
GOTLBO	1.0305	3.5214	1.1978	984.6560	48.6860
ITLBO	1.0305	3.4823	1.2013	981.9823	48.6428
RTLBO	1.0305	3.5033	1.2006	988.5601	48.6660
SATLBO	1.0307	3.3927	1.2308	952.6635	48.5435
LETLBO	1.0305	3.4827	1.2084	981.9822	48.6522
BSA	1.0306	3.2292	1.2118	994.3068	48.3503
TLABC	1.0306	3.4715	1.2017	972.9357	48.6313
IWOA	1.0305	3.4218	1.2113	983.9964	48.6523
IJAYA	1.0305	3.4703	1.2016	977.3752	48.6298

Table 11
Extracted parameters for the STM6-40/36 module.

Algorithm	Parameter				
	I_{ph} (A)	I_{sd} (μA)	R_s (Ω)	R_{sh} (Ω)	n
GSK	1.6635	1.9240	0.0040	16.5546	1.5315
ABC	1.6412	2.8745	0.0054	38.0477	1.5848
BBO	1.6311	3.4991	0.0024	18.4601	2.0934
DE	1.6635	2.0741	0.0037	16.8047	1.5395
JAYA	1.6663	3.4952	0.0024	25.3975	1.6006
PSO	1.6856	2.1695	0.0026	23.2751	1.8589
WOA	1.6627	2.0451	0.0044	23.4567	1.5709
TLBO	1.6606	3.2311	0.0026	23.3754	1.5911
GOTLBO	1.6631	2.3475	0.0031	17.4323	1.5536
ITLBO	1.6639	1.7610	0.0042	15.9420	1.5217
RTLBO	1.6639	1.7024	0.0043	15.8288	1.5180
SATLBO	1.6629	2.4954	0.0031	18.0761	1.5611
LETLBO	1.6634	1.6559	0.0042	16.9157	1.4879
BSA	1.6601	1.2069	0.0043	15.9283	1.5203
TLABC	1.7000	1.6338	0.0050	15.4001	1.5002
IWOA	1.7001	1.4127	0.0051	15.4001	1.5206
IJAYA	1.6646	1.4311	0.0049	14.9289	1.5446

Table 12
Extracted parameters for the STP6-120/36 module.

Algorithm	Parameter				
	I_{ph} (A)	I_{sd} (μA)	R_s (Ω)	R_{sh} (Ω)	n
GSK	7.4725	2.3350	0.0046	22.2199	1.2601
ABC	7.5395	49.6525	0.0027	56.2165	1.5809
BBO	7.4839	45.1002	0.0094	13.0576	1.6816
DE	7.4708	2.5614	0.0046	28.8094	1.2657
JAYA	7.5205	6.9255	0.0041	84.3610	1.3574
PSO	7.2404	3.7145	0.0046	29.9576	1.1455
WOA	7.3482	3.8812	0..0038	11.1193	1.5438
TLBO	7.5227	2.2956	0.0037	18.2979	1.4221
GOTLBO	7.4563	2.2559	0.0045	22.4749	1.2566
ITLBO	7.4725	2.3350	0.0046	22.2199	1.2601
RTLBO	7.4728	2.3167	0.0046	21.6438	1.2594
SATLBO	7.5356	2.6569	0.0045	24.3882	1.3214
LETLBO	7.4566	2.3396	0.0041	22.3654	1.2963
BSA	7.5229	3.3772	0.0030	23.2256	1.5321
TLABC	7.5611	3.4715	0..0049	23.6694	1.2698
IWOA	7.9547	3.4218	0.0036	22.5413	1.3849
IJAYA	7.4962	3.4703	0.0047	22.9846	1.4978

(1.44E−16). Then from Fig. 15, GSK also has a faster convergence rate in early stage and finds the global optimal value eventually.

- No matter in terms of RMSE value or convergence curve, GSK can get better results than other algorithms. In the case of relatively small number of fitness evaluations, applying the GSK algorithm to the parameter extraction of the PV module model can effectively obtain the global optimal value, which shows that the GSK algorithm has high parameter extraction accuracy and excellent convergence performance.

Table 13
The RMSE values of different algorithms in the Photowatt-PW201 module.

Algorithm	RMSE			
	Best	Worst	Mean	Std
GSK	**2.4251E−03**	**2.4251E−03**	**2.4251E−03**	1.04E−09
ABC	2.4262E−03	2.9456E−03	2.6178E−03	2.52E−04
BBO	2.5709E−03	2.7515E−02	1.0284E−02	7.29E−03
DE	**2.4251E−03**	2.5767E−03	2.4364E−03	1.25E−05
JAYA	2.4296E−03	2.5285E−03	2.4631E−03	2.33E−05
PSO	2.4255E−03	3.8889E−03	2.7226E−03	4.03E−04
WOA	2.6039E−03	8.9553E−02	1.9935E−02	2.19E−02
TLBO	2.4278E−03	1.5552E−02	3.5692E−03	2.60E−03
GOTLBO	2.4255E−03	5.8606E−03	2.7258E−03	7.25E−04
ITLBO	**2.4251E−03**	**2.4251E−03**	**2.4251E−03**	**3.46E−14**
RTLBO	**2.4251E−03**	2.9981E−03	2.5413E−03	4.98E−05
SATLBO	2.4257E−03	2.7099E−03	2.5024E−03	6.42E−05
BSA	2.4279E−03	2.6173E−03	2.4872E−03	3.98E−05
TLABC	**2.4251E−03**	2.9776E−03	2.4856E−03	1.12E−04

Table 14
The RMSE values of different algorithms in the STM6-40/36 module.

Algorithm	RMSE			
	Best	Worst	Mean	Std
GSK	**1.7298E−03**	**1.7298E−03**	**1.7298E−03**	**6.25E−18**
ABC	2.5535E−02	3.0767E−02	3.0201E−02	9.06E−04
BBO	2.1486E−02	2.3026E−01	8.3437E−02	5.36E−02
DE	1.7738E−03	3.0774E−03	2.1503E−03	2.89E−04
JAYA	2.0524E−03	5.3309E−03	3.1513E−03	8.39E−04
PSO	6.7718E−03	3.2947E−01	1.4209E−01	1.48E−01
WOA	3.2559E−03	3.4869E−02	1.5102E−02	9.99E−03
TLBO	1.7609E−03	2.7274E−02	5.0340E−03	4.55E−03
GOTLBO	1.8467E−03	3.3823E−03	2.7718E−03	3.41E−04
ITLBO	**1.7298E−03**	1.9172E−03	1.7407E−03	3.47E−05
RTLBO	**1.7298E−03**	2.9934E−03	1.9012E−03	2.29E−04
SATLBO	2.5673E−03	5.4962E−03	3.8456E−03	7.01E−04
BSA	4.8230E−03	1.5276E−02	1.1272E−02	2.51E−03
TLABC	**1.7298E−03**	2.4355E−03	2.0021E−03	2.04E−04

Table 15
The RMSE values of different algorithms in the STP6-120/36 module.

Algorithm	RMSE			
	Best	Worst	Mean	Std
GSK	**1.6601E−02**	**1.6601E−02**	**1.6601E−02**	**1.44E−16**
ABC	5.4466E−02	5.5223E−02	5.5149E−02	1.40E−04
BBO	3.9205E−01	1.5879E−00	1.3026E−00	2.87E−01
DE	1.6625E−02	3.4221E−02	2.2284E−02	5.13E−03
JAYA	1.7567E−02	7.7437E−02	2.3007E−02	1.05E−02
PSO	1.7518E−02	1.7047E−00	1.1944E−00	6.61E−01
WOA	2.0800E−02	1.4142E−00	9.8452E−02	2.53E−01
TLBO	1.7112E−02	5.1957E−02	3.5643E−02	1.03E−02
GOTLBO	1.6683E−02	3.0365E−02	2.1581E−02	3.45E−03
ITLBO	**1.6601E−02**	2.5833E−02	1.7081E−02	1.77E−03
RTLBO	1.6607E−02	2.0798E−02	1.7031E−02	8.16E−04
SATLBO	1.9893E−02	4.0081E−02	2.9798E−02	5.68E−03
BSA	2.8342E−02	5.2030E−02	4.6343E−02	5.31E−03
TLABC	1.6701E−02	1.8988E−02	1.7271E−02	5.70E−04

According to the RMSE values of the above algorithms in each PV module, five better algorithms were selected for comparison with GSK from them. In the Photowatt-PW201 module, we select DE, JAYA, ITLBO, BSA, and TLABC, and in the STM6-40/36 module and STP6-120/36 module, we select DE, GOTLBO, RTLBO, ITLBO, and TLABC. Then Tables 16, 17, 18 reveal the calculated current data obtained by these algorithms respectively. It can be seen that the GSK algorithm obtains the optimal IAE values in all three PV modules.

Table 16
The IAE results for the Photowatt-PW201 module.

Item	V_L (V)	$I_{L\,measured}$ (A)	$I_{L\,calculated}$ (A)					
			GSK	DE	JAYA	ITLBO	BSA	TLABC
1	0.1248	1.0315	1.0291	1.0291	1.0291	1.0291	1.0291	1.0291
2	1.8093	1.0300	1.0274	1.0274	1.0274	1.0274	1.0274	1.0274
3	3.3511	1.0260	1.0257	1.0257	1.0257	1.0257	1.0257	1.0257
4	4.7622	1.0220	1.0240	1.0240	1.0240	1.0240	1.0240	1.0240
5	6.0538	1.0180	1.0221	1.0221	1.0221	1.0221	1.0221	1.0220
6	7.2364	1.0155	1.0194	1.0194	1.0194	1.0194	1.0194	1.0192
7	8.3189	1.0140	1.0149	1.0149	1.0149	1.0149	1.0149	1.0147
8	9.3097	1.0100	1.0072	1.0072	1.0072	1.0072	1.0072	1.0068
9	10.2163	1.0035	1.0007	1.0007	1.0007	1.0007	1.0009	1.0009
10	11.0449	0.9880	0.9847	0.9847	0.9869	0.9847	0.9936	0.9868
11	11.8018	0.9630	0.9610	0.9610	0.9635	0.9610	0.9681	0.9635
12	12.4929	0.9255	0.9231	0.9231	0.9209	0.9231	0.9250	0.9239
13	13.1231	0.8725	0.8727	0.8727	0.8723	0.8728	0.8754	0.8702
14	13.6983	0.8075	0.8073	0.8073	0.8108	0.8071	0.8109	0.8079
15	14.2221	0.7265	0.7280	0.7280	0.7253	0.7282	0.7244	0.7225
16	14.6995	0.6345	0.6365	0.6365	0.6333	0.6367	0.6335	0.6373
17	15.1346	0.5345	0.5357	0.5357	0.5349	0.5359	0.5339	0.5378
18	15.5311	0.4275	0.4288	0.4289	0.4286	0.4289	0.4258	0.4225
19	15.8929	0.3185	0.3187	0.3187	0.3156	0.3191	0.3173	0.3199
20	16.2229	0.2085	0.2079	0.2079	0.2133	0.2078	0.2072	0.2094
21	16.5241	0.1010	0.0980	0.0981	0.1001	0.1001	0.1002	0.1021
22	16.7987	−0.0080	−0.0082	−0.0082	−0.0083	−0.0084	−0.0083	−0.0088
23	17.0499	−0.1110	−0.1109	−0.1114	−0.1101	−0.1114	−0.1115	−0.1122
24	17.2793	−0.2090	−0.2091	−0.2093	−0.2086	−0.2096	−0.2121	−0.2101
25	17.4885	−0.3030	−0.3020	−0.3041	−0.3036	−0.3034	−0.3035	−0.3014
	$\sum IAE$	–	0.0411	0.0417	0.0462	0.0409	0.0522	0..0507

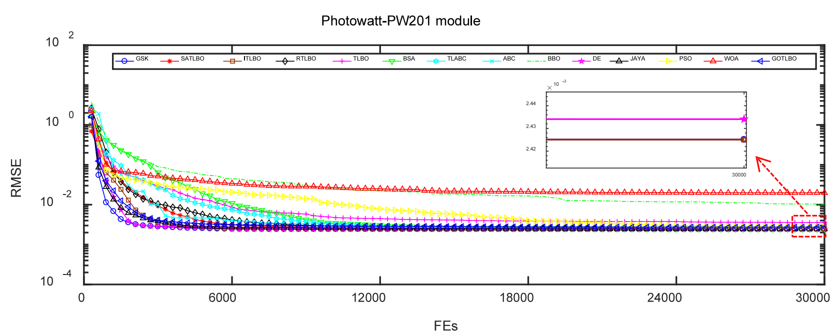

Fig. 13. The convergence curve for the Photowatt-PW201 module.

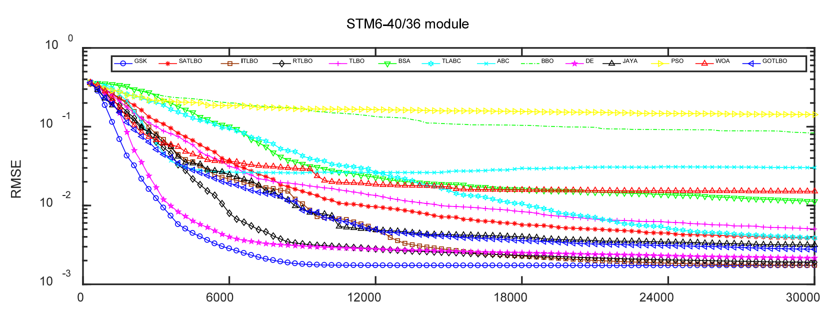

Fig. 14. The convergence curve for the STM6-40/36 module.

4.5. Whole performance

In the above three subsections, the GSK algorithm is compared and analyzed with other algorithms through single model statistical analysis methods. When we want to comprehensively validate the performance of the GSK algorithm, referring to the literature (García et al., 2009), we need to perform a multi-model statistical analysis on the models involved. Therefore, a Friedman test with a confidence of 0.05 is used to verify the general performance of GSK in this subsection. As shown in Fig. 16, GSK is obviously ranked the first, followed by ITLBO, RTLBO, DE, TLABC, JAYA, GOTLBO, BSA, SATLBO, ABC, TLBO, PSO, WOA, and BBO. The result shows that the general performance of the GSK algorithm in the PV model parameter extraction is extraordinarily excellent.

4.6. Discussions

In order to extract the parameters of PV models more effectively, this paper applies the GSK algorithm to this problem

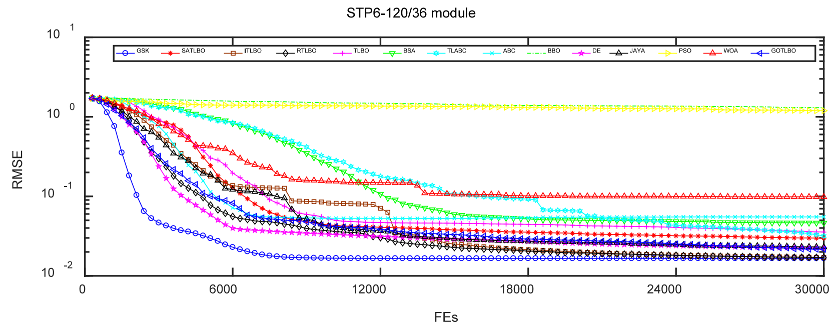

Fig. 15. The convergence curve for the STP6-120/36 module.

Table 17
The IAE results for the STM6-40/36 module.

Item	V_L (V)	$I_{L\,measured}$ (A)	$I_{L\,calculated}$ (A)					
			GSK	DE	GOTLBO	ITLBO	RTLBO	TLABC
1	0.0000	1.6630	1.6629	1.6626	1.6628	1.6635	1.6635	1.6626
2	0.1180	1.6630	1.6626	1.6624	1.6626	1.6633	1.6633	1.6624
3	2.2370	1.6610	1.6595	1.6592	1.6592	1.6595	1.6595	1.6592
4	5.4340	1.6530	1.6539	1.6542	1.6541	1.6539	1.6538	1.6542
5	7.2600	1.6500	1.6507	1.6512	1.6510	1.6506	1.6505	1.6512
6	9.6800	1.6450	1.6457	1.6464	1.6461	1.6454	1.6453	1.6464
7	11.5900	1.6400	1.6395	1.6405	1.6339	1.6392	1.6391	1.6403
8	12.6000	1.6360	1.6340	1.6337	1.6343	1.6337	1.6336	1.6347
9	13.3700	1.6290	1.6275	1.6275	1.6278	1.6273	1.6272	1.6281
10	14.0900	1.6190	1.6184	1.6197	1.6186	1.6183	1.6183	1.6188
11	14.8800	1.5970	1.6030	1.6031	1.6038	1.6031	1.6031	1.6032
12	15.5900	1.5810	1.5814	1.5815	1.5813	1.5816	1.5816	1.5813
13	16.4000	1.5420	1.5419	1.5415	1.5418	1.5423	1.5425	1.5415
14	16.7100	1.5240	1.5208	1.5213	1.5206	1.5213	1.5214	1.5218
15	16.9800	1.5000	1.4987	1.4981	1.4986	1.4993	1.4994	1.4982
16	17.1300	1.4850	1.4847	1.4838	1.4847	1.4853	1.4855	1.4843
17	17.3200	1.4650	1.4651	1.4628	1.4653	1.4657	1.4659	1.4647
18	17.9100	1.3880	1.3870	1.3861	1.3875	1.3878	1.3879	1.3870
19	19.0800	1.1180	1.1182	1.1201	1.1204	1.1188	1.1188	1.1203
20	21.0200	0.0000	−0.0003	0.0005	−0.0060	−0.0002	0.0001	0.0003
	$\sum IAE$	–	0.0218	0.0312	0.0366	0.0223	0.0225	0.0249

Table 18
The IAE results for the STP6-120/36 module.

Item	V_L (V)	$I_{L\,measured}$ (A)	$I_{L\,calculated}$ (A)					
			GSK	DE	GOTLBO	ITLBO	RTLBO	TLABC
1	0.0000	7.4800	7.4709	7.4942	7.4548	7.4709	7.4712	7.4942
2	9.0600	7.4500	7.4469	7.4683	7.4367	7.4469	7.4525	7.4683
3	9.4700	7.4200	7.4493	7.4319	7.4336	7.4493	7.4493	7.4319
4	10.3200	7.4400	7.4390	7.4284	7.4236	7.4390	7.4390	7.4284
5	11.1700	7.4100	7.4202	7.4151	7.4053	7.4202	7.4202	7.4151
6	11.8100	7.3800	7.3958	7.3903	7.3815	7.3958	7.3958	7.3903
7	12.3600	7.3700	7.3631	7.3864	7.3497	7.3631	7.3633	7.3864
8	12.7400	7.3400	7.3313	7.3553	7.3186	7.3312	7.3314	7.3563
9	13.1600	7.2900	7.2839	7.3043	7.2722	7.2839	7.2840	7.2868
10	13.5900	7.2300	7.2175	7.2114	7.2071	7.2175	7.2176	7.2174
11	14.1700	7.1000	7.0877	7.0883	7.0798	7.0882	7.0879	7.0883
12	14.5800	6.9700	6.9579	6.9556	6.9521	6.9581	6.9586	6.9556
13	14.9300	6.8300	6.8142	6.8101	6.8104	6.8143	6.8145	6.8201
14	15.3900	6.5800	6.5671	6.5662	6.5663	6.5671	6.5674	6.5683
15	15.7100	6.3600	6.3477	6.3478	6.3491	6.3477	6.3481	6.3479
16	16.0800	6.0000	6.0363	6.0219	6.0399	6.0364	6.0367	6.0343
17	16.3400	5.7500	5.7755	5.7693	5.7805	5.7761	5.7758	5.7693
18	16.7600	5.2700	5.2723	5.2802	5.2786	5.2726	5.2725	5.2802
19	16.9000	5.0700	5.0804	5.0886	5.0868	5.0805	5.0806	5.0804
20	17.1000	4.7900	4.7843	4.8031	4.7904	4.7843	4.7843	4.7982
21	17.2500	4.5600	4.5447	4.5446	4.5504	4.5446	4.5447	4.5447
22	17.4100	4.2900	4.2724	4.3008	4.2772	4.2725	4.2722	4.2815
23	17.6500	3.8300	3.8307	3.8315	3.8335	3.8306	3.8304	3.8309
24	19.2100	0.0000	0.0010	0.0096	0.0035	0.0012	0.0009	0.0021
	$\sum IAE$	–	0.2829	0.3284	0.3650	0.2834	0.2874	0.2889

and compares it with other algorithms. Through the experimental results, we can summarize as follows:

(i) The population size does affect the performance of GSK. Therefore, to show the algorithm performance of GSK in

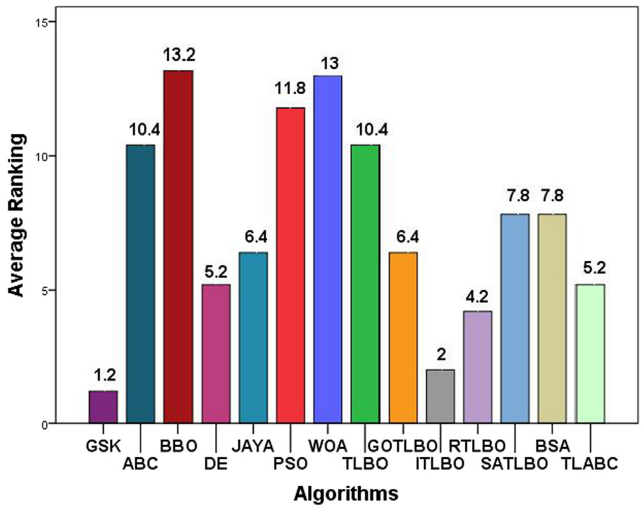

Fig. 16. Friedman test result.

the PV model parameter extraction problem effectively, the *NP* value is set to a moderate value, e.g., 30 for testing in this paper. If the *NP* value is higher or lower than 30, the performance becomes worse and worse.

(ii) From the I–V and P-V characteristic curves, it can be obtained that GSK can achieve reliable and accurate values in the parameter extraction problem of different PV models.

(iii) The convergence curves of the SDM and DDM show that GSK has a slow convergence speed in the initial stage. However, it can jump out of local optima and converge to the smallest RMSE value eventually. It indicates that GSK has superior convergence performance.

(iv) Comparing with other advanced optimization algorithms, GSK can obtain optimal values in all RMSE metrics and IAE, indicating that this algorithm performs competitively in terms of convergence performance and parameter extraction accuracy. It is worth mentioning that ITLBO can obtain a smaller standard deviation value than GSK in the Photowatt-PW201 module, which shows that the accuracy of GSK on this PV model needs to be improved.

(v) Through the Friedman test to comprehensively validate the performance of GSK, the result shows that the general performance of GSK in the PV model parameter extraction is extraordinarily excellent.

5. Conclusion

GSK is a new metaheuristic algorithm and is easy to implement. In this paper, GSK is applied to solve the PV model parameter extraction problem. To better verify the effectiveness of this algorithm, it is applied to the single diode model, double diode model, and three PV module models (the Photowatt-PWP201 module, STM6-40/36 module, and STP6-120/36 module). The results show that the population size does have impact on the performance of GSK. A moderate value 30 is recommended for the solved problem. Moreover, compared with other basic metaheuristic algorithms and advanced metaheuristic algorithms, GSK can obtain overall smaller RMSE values with better robustness and convergence. In summary, GSK has excellent performance and strong competitiveness in the PV model parameter extraction.

In future, the basic GSK algorithm will be improved using parameter self-adapting strategies to further ameliorate its performance in solving this involved problem and MPPT problem.

CRediT authorship contribution statement

Guojiang Xiong: Conceptualization, Methodology, Writing - review & editing. **Lei Li:** Software, Writing - original draft. **Ali Wagdy Mohamed:** Resources, Writing - review & editing. **Xufeng Yuan:** Formal analysis, Validation. **Jing Zhang:** Formal analysis, Validation.

Declaration of competing interest

The authors declare that they have no known competing financial interests or personal relationships that could have appeared to influence the work reported in this paper.

Acknowledgments

The authors would like to thank the editor and the reviewers for their constructive comments. This work was supported by the National Natural Science Foundation of China (Grant No. 51907035, 51867005), the Guizhou Education Department Growth Foundation for Youth Scientific and Technological Talents, China (Grant No. QianJiaoHe KY Zi [2018]108).

References

Abbassi, Rabeh, Abbassi, Abdelkader, Heidari, Ali Asghar, Mirjalili, Seyedali, 2019. An efficient salp swarm-inspired algorithm for parameters identification of photovoltaic cell models. Energy Convers. Manage. 179, 362–372.

Abbassi, Rabeh, Abbassi, Abdelkader, Jemli, Mohamed, Chebbi, Souad, 2018a. Identification of unknown parameters of solar cell models: A comprehensive overview of available approaches. Renew. Sustain. Energy Rev. 90, 453–474.

Abbassi, Abdelkader, Gammoudi, Rabiaa, Dami, Mohamed Ali, Hasnaoui, Othman, Jemli, Mohamed, 2018b. An improved single-diode model parameters extraction at different operating conditions with a view to modeling a photovoltaic generator: A comparative study. Sol. Energy 155, 478–489.

Ahmed, M. Aram, Rashid, Tarik A., Saeed, Ab Soran M., Gómez-Pulido, A. Juan, 2020. Cat swarm optimization algorithm: A survey and performance evaluation. Comput. Intell. Neurosci. 2020, 314–325.

Ali, E.E., El-Hameed, M.A., El-Fergany, A.A., El-Arini, M.M., 2016. Parameter extraction of photovoltaic generating units using multi-verse optimizer. Sustain. Energy Technol. Assess. 17, 68–76.

AlRashidi, M.R., AlHajri, M.F., El-Naggar, K.M., Al-Othman, A.K., 2011. A new estimation approach for determining the I-V characteristics of solar cells. Sol. Energy 85 (7), 1543–1550.

Aman, M.M., Solangi, K.H., Hossain, M.S., 2015. A review of safety. In: Health and Environmental (SHE) Issues of Solar Energy System, Vol. 41. pp. 1190–1204.

Askarzadeh, A., Rezazadeh, A., 2019. Parameter identification for solar cell models using harmony search based algorithms. Sol. Energy 86, 3241–3249.

Askarzadeh, Alireza, Santos Coelho, Leandro dos, 2015. Determination of photovoltaic modules parameters at different operating conditions using a novel bird mating optimizer approach. Energy Convers. Manage. 89, 608–614.

Ben, M.R., 2020. Extraction of uncertain parameters of single and double diode model of a photovoltaic panel using Salp Swarm algorithm. Measurement 154 (C), 437–449.

Brano, Valerio Lo, Ciulla, Giuseppina, 2013. An efficient analytical approach for obtaining a five parameters model of photovoltaic modules using only reference data. Appl. Energy 111 (111), 894–903.

Chan, D.S.H., Phillips, J.R., Phang, J.C.H., 1986. A comparative study of extraction methods for solar cell model parameters. Solid-State Electron. 29 (3), 329–337.

Chen, Xu, Xu, Bin, Mei, Congli, Ding, Yuhan, Li, Kangji, 2018. Teaching–learning–based artificial bee colony for solar photovoltaic parameter estimation. Appl. Energy 212, 1578–1588.

Chen, X., Yu, K., Du, W., Zhao, W., Liu, G., 2019. Parameters identification of solar cell models using generalized oppositional teaching learning based optimization. Energy 99, 170–180.

Chin, Vun Jack, Salam, Zainal, Ishaque, Kashif, 2015. Cell modelling and model parameters estimation techniques for photovoltaic simulator application: A review. Appl. Energy 154, 500–519.

Civicioglu, Pinar, 2013. Backtracking search optimization algorithm for numerical optimization problems. Appl. Math. Comput. 219, 8121–8144.

Cuce, E., Cuce, P.M., Karaka, I.H., Bali, T., 2017. An accurate model for photovoltaic (PV) modules to determine electrical characteristics and thermodynamic performance parameters. Energy Convers. Manage. 146, 205–216.

Derick, M., Rani, C., Rajesh, M., Farrag, M.E., Wang, Y., Busawon, K., 2017. An improved optimization technique for estimation of solar photovoltaic parameters. Sol. Energy 157, 116–124.

Easwarakhanthan, T., Bottin, J., Bouhouch, I., Boutrit, C., 1986. Nonlinear minimization algorithm for determining the solar cell parameters with microcomputers. Int. J. Sustain. Energy 4 (1), 1–12.

Elbaset, Adel A., Ali, Hamdi, Abd-El Sattar, Montaser, 2014. Novel seven-parameter model for photovoltaic modules. Sol. Energy Mater. Sol. Cells 130, 442–455.

Elkholy, A., El-Ela, A., 2019. Optimal parameters estimation and modelling of photovoltaic modules using analytical method. Heliyon 5 (7), 123-144.

Fathy, Ahmed, Rezk, Hegazy, 2017. Parameter estimation of photovoltaic system using imperialist competitive algorithm. Renew. Energy 111, 307–320.

Franco, R.A.P., Vieira, F.H.T., 2018. Analytical method for extraction of the single-diode model parameters for photovoltaic panels from datasheet data. Electron. Lett. 54 (8), 519–521.

García, S., Molina, D., Lozano, M., Herrera, F., 2009. A study on the use of non-parametric tests for analyzing the evolutionary algorithm' behaviour: a case study on the CEC' 2005 special session on real parameter optimization. J. Heuristics 15 (6), 617–644.

Ghani, F., Rosengarten, G., Duke, M., Carson, J.K., 2014. The numerical calculation of single diode solar-cell modelling parameters. Renew. Energy 72, 105–112.

Hamid, Naima, Abounacer, Rachida, Oumhand, Mohammed Idali, Feddaoui, M'barek, Agliz, Driss, 2018. Parameters Identification of Photovoltaic Solar Ccells and Module Using the Genetic Algorithm with Convex Combination Crossover, Vol. 40. Taylor & Francis, pp. 517–524, (5).

Hao, Sun, Hilmi, Luş, Raimondo, Betti, 2013. Identification of structural models using a modified Artificial Bee Colony algorithm. Comput. Struct. 116, 59–74.

Hultmann Ayala, H.V., Coelho, L.D.S., Mariani, V.C., Askarzadeh, A., 2015. An improved free search differential evolution algorithm: A case study on parameters identification of one diode equivalent circuit of a solar cell module. Energy 93, 1515–1522.

International Energy Agency Meetings, 2020. Fed. Regist. / FIND 85 (115).

Jordehi, A.R., 2016. Parameter estimation of solar photovoltaic (PV) cells: A review. Renew. Sustain. Energy Rev. 61, 134–142.

Karaboga, D., Ozturk, C., 2011. A novel clustering approach: Artificial Bee Colony (ABC) algorithm. Appl. Soft Comput. 11, 652–657.

Kennedy, J., Eberhart, R.C., 1995. Particle swarm optimization. In: Proceedings of the IEEE International Conference on Neural Networks. IEEE, Perth, Australia, pp. 1942–1948.

Li, Yuan, Huang, Wenxiao, Huang, Huihui, Hewitt, Corey, Chen, Yonghua, Fang, Guojia, Carroll, David L., 2013. Evaluation of methods to extract parameters from current–voltage characteristics of solar cells. Sol. Energy 90, 654–659.

Li, G., Qiu, S., 2018. Parameters extraction method for solar photovoltaic module. In: 2018 IEEE International Power Electronics and Application Conference and Exposition (PEAC). Shenzhen. pp. 1–4.

Lin, P., Cheng, S., Yeh, W., Chen, Z., Wu, L., 2017. Parameters extraction of solar cell models using a modified simplified swarm optimization algorithm. Sol. Energy 144, 594–603.

Lun, S., Du, C., Sang, J., et al., 2014. An improved explicit I–V model of a solar cell based on symbolic function and manufacturer's datasheet. Sol. Energy 110, 603–614.

Messaoud, Ramzi Ben, 2020a. Extraction of uncertain parameters of single-diode model of a photovoltaic panel using simulated annealing optimization. 6, 350–357.

Messaoud, R.B., 2020b. Extraction of uncertain parameters of double-diode model of a photovoltaic panel using Ant Lion Optimization. SN Appl. Sci. 2 (2), 367–372.

Messaoud, R.B., 2020c. Extraction of uncertain parameters of single-diode model of a photovoltaic panel using simulated annealing optimization. Energy Rep. 6 (2020), 350–357.

Mirjalili, Seyedali, Lewis, Andrew, 2016. The whale optimization algorithm. Adv. Eng. Softw. 95, 51–67.

Mohamed, Ali Wagdy, Hadi, Anas A., Mohamed, Ali Khater, 2020. Gaining-sharing knowledge based algorithm for solving optimization problems: a novel nature-inspired algorithm. Int. J. Mach. Learn. Cybern. 11, 1501–1529.

Mohammed, R.H., Asghar, H.A., Mingjing, W., Huiling, C., 2019. Boosted Mutation-Based Harris Hawks Optimizer for Parameters Identification of Single-Diode Solar Cell Models, Vol. 209. Elsevier Ltd, pp. 146–155.

Oliva, Diego, Aziz, Mohamed Abd El, Hassanien, Aboul Ella, 2017. Parameter estimation of photovoltaic cells using an improved chaotic whale optimization algorithm. Appl. Energy 200, 141–154.

Ortiz-Conde, A., García Sánchez, F.J., Muci, J., 2016. New method to extract the model parameters of solar cells from the explicit analytic solutions of their illuminated I–V characteristics. Solar Energy Mater. Solar Cells 90, 352–361.

Phang, J.C.H., Chan, D.S.H., Phillips, J.R., 1984. Accurate analytical method for the extraction of solar cell model parameters. Electron. Lett. 20 (10), 406–408.

Rajasekar, N., Kumar, Neeraja Krishna, Venugopalan, Rini, 2013. Bacterial foraging algorithm based solar PV parameter estimation. Sol. Energy 97, 255–265.

Rao, R., 2016. Jaya: a simple and new optimization algorithm for solving constrained and unconstrained optimization problems. Int. J. Ind. Eng. Comput. 7, 19–34.

Rao, R.V., Patel, V., 2013. An improved teaching-learning-based optimization algorithm for solving unconstrained optimization problems. Sci. Iran. Trans. D: Comput. Sci. Eng. Electr. Eng. 20 (3), 710–720.

Rao, R.V., Savsani, V.J., Vakharia, D.P., 2011. Teaching–learning-based optimization: An optimization method for continuous non-linear large scale problems. Inform. Sci. 183 (1), 1–15.

Rezaee Jordehi, A., 2018. Enhanced leader particle swarm optimisation (ELPSO): An efficient algorithm for parameter estimation of photovoltaic (PV) cells and modules. Sol. Energy 159, 78–87.

Rusirawan, D., Farkas, I., 2014. Identification of Model Parameters of the Photovoltaic Solar Cells, Vol. 57. Elsevier Ltd, pp. 39–46.

Sharma, Anurag, 2016. Solar energy a present & future energy solution. Invertis J. Renew. Energy 6 (4).

Simon, D., 2008. Biogeography-based optimization. IEEE Trans. Evol. Comput. 70, 2–713.

Srihari, G., Chandra, J.K., 2020. Parameter extraction of photovoltaic cell using an improved cuckoo search optimization. Sol. Energy 204, 280–293.

Storn, Rainer, Price, Kenneth, 1997. Differential evolution – A simple and efficient heuristic for global optimization over continuous spaces. J. Global Optim. 11 (4), 341–359.

Stornelli, Vincenzo, Muttillo, Mirco, Rubeis, Tullio de, et al., 2019. A new simplified five-parameter estimation method for single-diode model of photovoltaic panels. 12 (22).

Toledo, F.J., Blanes, J.M., 2014. Geometric properties of the single-diode photovoltaic model and a new very simple method for parameters extraction. Renew. Energy 72, 125–133.

Tong, Nhan Thanh, Pora, Wanchalerm, 2016. A parameter extraction technique exploiting intrinsic properties of solar cells. Appl. Energy 176, 104–115.

Tooryan, Fatemeh, Fard, Hamid Hassanzadeh, Collins, Edward R., Jin, Shuangshuang, Ramezani, Bahram, 2020. Smart integration of renewable energy resources, electrical, and thermal energy storage in microgrid applications. Energy 212.

Wenchao, Yi, Yinzhi, Zhou, Liang, Gao, Xinyu, Li, Jianhu, Mou, 2016. An improved adaptive differential evolution algorithm for continuous optimization. Expert Syst. Appl. 44, 1–12.

Wolpert, D.H., Macready, W.G., 1997. No free lunch theorems for optimization. IEEE Trans. Evol. Comput. 1 (1), 67–82.

Xiong, Guojiang, Zhang, Jing, Shi, Dongyuan, He, Yu, 2018a. Parameter identification of solid oxide fuel cells with ranking teaching-learning based algorithm. Energy Convers. Manage. 174, 126–137.

Xiong, Guojiang, Zhang, Jing, Shi, Dongyuan, et al., 2018b. Parameter extraction of solar photovoltaic models using an improved whale optimization algorithm. Energy Convers. Manage. 174, 388–405.

Xiong, Guojiang, Zhang, Jing, Shi, Dongyuan, et al., 2019a. Application of supply-demand-based optimization for parameter extraction of solar photovoltaic models. Complexity 1–21.

Xiong, Guojiang, Zhang, Jing, Shi, Dongyuan, et al., 2019b. Modified search strategies assisted crossover whale optimization algorithm with selection operator for parameter extraction of solar photovoltaic models. Remote Sens. 11 (23).

Xiong, Guojiang, Zhang, Jing, Shi, Dongyuan, et al., 2020a. Parameter extraction of solar photovoltaic models with an either-or teaching learning based algorithm. Energy Convers. Manage. 224.

Xiong, Guojiang, Zhang, Jing, Shi, Dongyuan, et al., 2020b. Winner-leading competitive swarm optimizer with dynamic Gaussian mutation for parameter extraction of solar photovoltaic models. Energy Convers. Manage. 206.

Xiong, Guojiang, Zhang, Jing, Yuan, Xufeng, et al., 2018c. Application of symbiotic organisms search algorithm for parameter extraction of solar cell models. Appl. Sci. 8 (11).

Xiong, Guojiang, et al., 2020c. Winner-leading competitive swarm optimizer with dynamic Gaussian mutation for parameter extraction of solar photovoltaic models. Energy Convers. Manage. 206.

Yang, Qian, 2020. Discussion on the application of new energy photovoltaic power generation system. Int. J. New Dev. Eng. Soc. 24 (1), 216–220.

Yu, Kunjie, Chen, Xu, Wang, Xin, Wang, Zhenlei, 2017a. Parameters identification of photovoltaic models using self-adaptive teaching-learning-based optimization. Energy Convers. Manage. 145, 233–246.

Yu, K., Liang, J.J., Qu, B.Y., Chen, X., Wang, H., 2017b. Parameters identification of photovoltaic models using an improved JAYA optimization algorithm. Energy Convers. Manage. 150, 742–753.

Zou, Feng, Wang, Lei, Hei, Xinhong, Chen, Debao, 2015. Teaching–learning-based optimization with learning experience of other learners and its application. Appl. Soft Comput. 37, 725–736.